

1 **Distinct gene expression dynamics in germ line and somatic tissue during ovariole**  
2 **morphogenesis in *Drosophila melanogaster***

3 Shreeharsha Tarikere<sup>1a</sup>, Guillem Ylla<sup>1a</sup> and Cassandra G. Extavour<sup>1, 2\*</sup>

4

5 1. Department of Organismic and Evolutionary Biology, Harvard University

6 2. Department of Molecular and Cellular Biology, Harvard University

7

8 \* Author for correspondence: [extavour@oeb.harvard.edu](mailto:extavour@oeb.harvard.edu)

9 a. These authors contributed equally to this work

10

11

## 12 **Abstract**

13 The survival and evolution of a species is a function of the number of offspring it can  
14 produce. In insects the number of eggs that an ovary can produce is a major determinant  
15 of reproductive capacity. Insect ovaries are made up of tubular egg-producing subunits  
16 called ovarioles, whose number largely determines the number of eggs that can be  
17 potentially laid. Ovariole number is directly determined by the number of cellular  
18 structures called terminal filaments, which are stacks of cells that assemble in the larval  
19 ovary. Elucidating the developmental and regulatory mechanisms of terminal filament  
20 formation is thus key to understanding the regulation of insect reproduction through  
21 ovariole number regulation. We systematically measured mRNA expression of all cells in  
22 the larval ovary at the beginning, middle and end of terminal filament formation. We also  
23 separated somatic and germ line cells during these stages and assessed their tissue-  
24 specific gene expression during larval ovary development. We found that the number of  
25 differentially expressed somatic genes is highest during late stages of terminal filament  
26 formation and includes many signaling pathways that govern ovary development. We also  
27 show that germ line tissue, in contrast, shows greater differential expression during early  
28 stages of terminal filament formation, and highly expressed germ line genes at these  
29 stages largely control cell division and DNA repair. We provide a tissue-specific and  
30 temporal transcriptomic dataset of gene expression in the developing larval ovary as a  
31 resource to study insect reproduction.

32

33 **KEY WORDS:** Ovary, FACS, RNA-Seq, Terminal filament, Germ line, Stem cell niche.

## 34 INTRODUCTION

35 Healthy reproductive organs are among the most important factors that determine the  
36 fertility of an individual, and more importantly, continuity of the species itself. Reproductive  
37 fitness, including fecundity, is determined by the number of progenies an organism can  
38 produce. In insects, egg-producing subunits of ovaries are called ovarioles (BÜNING  
39 1994). In flies of the genus *Drosophila*, the number of ovarioles predicts the peak egg  
40 laying potential of the females of the species (DAVID 1970), and is negatively correlated  
41 with egg size but positively correlated with reproductive output (CHURCH *et al.* 2021). The  
42 number of ovarioles varies widely across insects and is in the range of 18-24 ovarioles  
43 per ovary in wild type North American populations of *Drosophila melanogaster* (HONEK  
44 1993; MARKOW AND O'GRADY 2007; HODIN 2009). In *Drosophila*, adult ovariole number is  
45 established in the larval stages through the development of a species-specific number of  
46 linear somatic cell stacks called terminal filaments (KING *et al.* 1968). The number of  
47 terminal filaments assembled by the time of pupariation usually predicts adult ovariole  
48 number (KING 1970; HODIN AND RIDDIFORD 2000a). Thus, terminal filaments are the  
49 primordial larval structures whose number ultimately determines ovariole number. The  
50 genetic mechanisms governing ovary morphogenesis, which includes the process of  
51 regulation of terminal filament number and assembly during larval ovary development,  
52 remain poorly understood.

53 Ovary morphogenesis is orchestrated by interactions of the cell types of somatic  
54 and germ line tissues. Larval somatic ovarian tissue is principally made up of five cell  
55 types - sheath cells, swarm cells, terminal filaments, cap cells, and intermingled cells. The  
56 anterior most cells of the ovary are the sheath cells, and a sub-population of these apically

57 positioned cells undergo two cell migration events during larval ovary development. First,  
58 a population of sheath cells called swarm cells migrates from the anterior to the posterior  
59 of the ovary to form the basal region in the mid third larval instar stage (COUDERC *et al.*  
60 2002; GREEN II AND EXTAVOUR 2012). Secondly, in the late third instar and early pupal  
61 stages, sheath cells migrate from the apical to the basal region, traversing in between  
62 terminal filaments (KING *et al.* 1968). These sheath cells lay down basement membrane  
63 in their path, which encapsulates developing ovarioles (KING 1970). Terminal filaments  
64 are stacks of cells located just below the sheath cells in the anterior larval ovary. They  
65 are formed by a process of progressive intercalation of flattened cells into stacks, and  
66 stack formation occurs in a “wave” that proceeds from the medial to the lateral side in the  
67 larval ovary (**Figure 1A**) (SAHUT-BARNOLA *et al.* 1995a).

68 The genes *bric á brac 1 (bab1)* and *bric á brac 2 (bab2)* are expressed in the  
69 terminal filaments and essential for terminal filament cell differentiation and terminal  
70 filament assembly (GODT AND LASKI 1995b; SAHUT-BARNOLA *et al.* 1995a; COUDERC *et al.*  
71 2002; SALER *et al.* 2020). The gene *engrailed* is also expressed in terminal filaments, and  
72 at a lower level in the cap cells of the larval ovary (BOLIVAR *et al.* 2006; SALER *et al.* 2020).  
73 Clones homozygous for an *engrailed* deletion allele generated in terminal filaments in  
74 third instar larvae showed that this gene is required in initial terminal filament precursors  
75 for the correct assembly of terminal filaments. (BOLIVAR *et al.* 2006). However, a  
76 subsequent study showed that RNAi knockdowns of *engrailed* and *invected* driven by  
77 *bab:GAL4* in larval terminal filament and cap cells does not affect terminal filament  
78 formation (SALER *et al.* 2020). This could mean that *engrailed/invected* are not absolutely  
79 required for terminal filament formation, but that genetic heterogeneity with respect to

80 *engrailed/invected* dose, is important among terminal filament precursor cells to ensure  
81 correct terminal filament morphogenesis. Accumulation of *engrailed* in terminal filaments  
82 is dependent on *bab* gene expression (SALER *et al.* 2020).

83 We previously showed that the *Hippo signaling* pathway controls the regulation of  
84 cell proliferation in somatic cells, thereby affecting the number of terminal filaments and  
85 their constituent terminal filament cells (SARIKAYA AND EXTAVOUR 2015). During early  
86 terminal filament formation, Actin and Armadillo (*arm*) proteins deposited in the region  
87 between terminal filaments make a scaffold to flatten and intercalate terminal filament  
88 cells (GODT AND LASKI 1995b; SAHUT-BARNOLA *et al.* 1995a; CHEN *et al.* 2001). Expression  
89 of the protein cofilin (*twinstar*) is required in terminal filament and apical cells for actin-  
90 based change in cell shape, and loss of cofilin causes a reduction in terminal filament and  
91 apical cell numbers (CHEN *et al.* 2001).

92 Normal growth of an ovary depends on the homeostatic proliferation of the somatic  
93 and germ line tissues (GILBOA AND LEHMANN 2006; GILBOA 2015). This balance between  
94 somatic and germ line tissue populations is achieved by regulation of proliferation,  
95 differentiation and apoptosis of stem cell populations of somatic and germ cell lineages  
96 (SAHUT-BARNOLA *et al.* 1995a; SAHUT-BARNOLA *et al.* 1996). Somatic cells called  
97 intermingled cells interact with the germ cells and control their proliferation (LI *et al.* 2003;  
98 GILBOA AND LEHMANN 2006; SARIKAYA AND EXTAVOUR 2015; LAI *et al.* 2017; PANCHAL *et al.*  
99 2017; LI *et al.* 2019). *Notch*, *hedgehog*, *Mitogen Activated Protein Kinase (MAPK)* and  
100 *Epidermal growth factor receptor (EGFR)* signaling pathways, as well as the transcription  
101 factor *traffic jam* maintain the germ line stem cell niche (BESSE *et al.* 2005; SONG *et al.*

102 2007; MATSUOKA *et al.* 2013; SARIKAYA AND EXTAVOUR 2015; YATSENKO AND SHCHERBATA  
103 2021), which is established at the base (posterior) of each terminal filament.

104 Recent work by Slaidina and colleagues used single-cell transcriptomics to  
105 describe the gene expression profiles of the various cell types of the late third instar larval  
106 ovary (SLAIDINA *et al.* 2020). They sub-divided terminal filament cells into anterior or  
107 posterior cell types, and sheath cells into migratory or non-migratory cell types, based on  
108 gene expression patterns of the single cell sub-populations. (SLAIDINA *et al.* 2020). While  
109 this study examined a single time point of ovary development, given that ovary  
110 morphogenesis is a temporal process, we hypothesize that changes in gene expression  
111 patterns over the course of development may be important to regulate morphogenesis.  
112 Thus, a gene expression study across the developing stages of larval ovary would  
113 advance our understanding of the transcriptomic regulation of ovarian morphogenesis.

114 Although all major conserved animal signaling pathways are known to be involved  
115 in ovarian morphogenesis (TWOMBLY *et al.* 1996; COHEN *et al.* 2002; HUANG *et al.* 2005;  
116 SONG *et al.* 2007; GANCZ AND GILBOA 2013; GREEN AND EXTAVOUR 2014; SARIKAYA AND  
117 EXTAVOUR 2015; KUMAR *et al.* 2020), a systematic gene expression profile of a developing  
118 ovary is lacking. Such system-wide gene expression data for the ovary throughout  
119 terminal filament morphogenesis, including the potentially distinct transcriptional profiles  
120 of germ cells and somatic cells, could shed light on the processes involved in the  
121 maintenance of cell types necessary to shape the ovary and control the number of  
122 ovarioles.

123 To this end, we measured gene expression during the development of the larval  
124 ovary by systematically staging and sequencing mRNA from whole ovaries before, during

125 and after terminal filament formation. Furthermore, we separated somatic and germ line  
126 tissue types at each of these stages to analyze tissue-specific gene expression. We  
127 compared the gene expression profiles across tissues and also across stages of ovary  
128 development. We then employed functional enrichment analysis to determine the different  
129 biological functions active in the three larval developmental stages and two tissue types  
130 that could yield information on ovary morphogenesis. This dataset is an important  
131 temporal and tissue specific gene expression resource for the insect developmental  
132 biology community to understand early ovary development.

133

## 134 **RESULTS**

### 135 **Staging larval ovary development during terminal filament formation**

136 We divided the developing *Drosophila* larval ovary into three stages during terminal  
137 filament formation and used RNA-seq to quantify gene expression at these stages  
138 (**Figure 1A**). First, we considered an early stage of terminal filament formation at the  
139 early third instar larva (72 hours After Egg Laying, 72h AEL), when terminal filament  
140 assembly is initiating (GODT AND LASKI 1995b) (**Figure 1A-i**). Second, we assigned the  
141 middle (mid) stage (96h AEL) as 24 hours after the early stage, at the midway point of  
142 terminal filament assembly (GODT AND LASKI 1995b) (**Figure 1A-ii**). Third, the late stage  
143 (120h AEL) was defined as the time point of white pupa formation (when the larvae  
144 become immobile at the larval to pupal transition (ASHBURNER *et al.* 2005)), which  
145 occurs 24 hours after the middle stage (**Figure 1A-iii**). At the white pupa stage, terminal  
146 filament assembly is complete and the number of terminal filaments reflects the number  
147 of adult ovarioles (HODIN AND RIDDIFORD 2000b) (**Figure 1B**).

148 We dissected these three stages of developing ovaries from larvae obtained from  
149 synchronized eggs and sequenced the transcripts present at each stage from pools of  
150 30-100 ovaries (**Supplementary Table S1**). We aligned reads to the *Drosophila*  
151 *melanogaster* genome (FlyBase v6.36), which yielded between 88.49% and 98.06% of  
152 reads aligned per sample (**Supplementary Figure S1, Supplementary Table S1**).  
153 Clustering analysis based on the variance-stabilizing transformation (VST) of the gene  
154 counts of each sample confirmed that the three biological replicates of each stage  
155 clustered together, and that the three stages were well separated, as reflected by the  
156 dendrogram of the hierarchical analysis and the principal component analysis (PCA)  
157 (**Figure 2A-B**). Furthermore, the dendrogram visualization of the hierarchical clustering  
158 results revealed that the mid stage was more similar in expression profile to the early  
159 stage than to the late stage. This indicates a more pronounced transcriptomic change at  
160 the transition from mid to late, than from early to mid, despite the fact that the same  
161 chronological amount of time had elapsed between each stage.

162

### 163 **Differential gene expression analysis of whole ovary samples at different stages**

164 We analyzed the transcriptional differences between each stage and the successive one,  
165 thus performing a differential expression analysis comparing early to mid and mid to late  
166 transitions, using DESeq2 (Love *et al.* 2014) with a threshold of  $p < 0.01$  (see Methods).  
167 We found a significantly higher number of genes differentially expressed in the mid to late  
168 transition (2,727 genes), than in the early to mid-transition (685) (**Figure 2C,**  
169 **Supplementary Table S2**). Interestingly, from early to mid stages twice as many genes  
170 were downregulated (480) as upregulated (205), while from mid to late stages

171 approximately the same proportion of genes were upregulated (1,264) and  
172 downregulated (1,463). We then identified the genes that were differentially expressed in  
173 one stage as compared to the other two stages, with the aim of revealing genes with  
174 stage-specific over- or under-expression. We found that early and late stages had many  
175 more over-expressed genes (1,434 and 1,626 respectively) than the mid stage (538)  
176 **(Figure 2D, Supplementary Table S3)**. A heatmap representing the expression levels  
177 of the stage-specific overexpressed genes clearly separates the three groups of genes  
178 **(Figure 2E)**. The first group in the heatmap contains the 1,478 genes that are highly  
179 expressed specifically at early stages, with less expression at mid stages and very low  
180 expression at the late stage. Another large group of 1,618 genes are highly expressed  
181 specifically at late stages and show low expression at early and mid stages. Finally, we  
182 identified a third and smallest group of 202 genes that are highly expressed at mid stages,  
183 with some detectable expression at early stages, but little detectable expression at the  
184 late stage **(Figure 2E)**. These results are consistent with our previous observation that  
185 there is a high gene expression similarity in early and mid-stages, and an increased  
186 transcriptomic change from mid to late stages.

187

### 188 **Separation of somatic and germ line tissues in the developing ovary**

189 Given our ultimate interest in gene regulatory functions and dynamics during terminal  
190 filament formation, we wished to understand the predicted functions of the many  
191 differentially expressed genes across stages. We reasoned, however, that given the  
192 different developmental numbers, roles and behaviors of germ line and somatic cells in  
193 this developing organ, considering functional categories of differentially expressed genes

194 in these whole ovary samples would be only minimally informative. We therefore designed  
195 an experimental strategy that allowed us to consider the transcriptional dynamics of the  
196 germ line and soma separately, described below.

197 To understand the gene expression differences between the somatic and germ  
198 line tissues of the ovary during terminal filament morphogenesis, we drove somatic and  
199 germ line tissue-specific GFP expression using the UAS-GAL4 system (BRAND AND  
200 PERRIMON 1993), using the drivers *bab:GAL4* and *nos:GAL4* respectively (see Methods).  
201 The paralogous genes *bab 1* and *bab 2* are expressed in somatic ovarian cells and are  
202 essential for terminal filament formation, differentiation of terminal filament cells and stem  
203 cell niche maintenance (SAHUT-BARNOLA *et al.* 1995b; COUDERC *et al.* 2002; SALER *et al.*  
204 20120). The two Bab proteins act in a synergistic and partially redundant fashion in the  
205 ovary, and mutations in the *bab* genes cause defects in terminal filament and ovariole  
206 number (GODT AND LASKI 1995a; SAHUT-BARNOLA *et al.* 1995a; COUDERC *et al.* 2002). The  
207 gene *bab1* is expressed strongly in the apical and terminal filaments of the larval ovary,  
208 while *bab2* is expressed in swarm cells, in addition to other somatic cells of the larval  
209 ovary (CABRERA *et al.* 2002; COUDERC *et al.* 2002). We used the *bab pGAL<sup>4-2</sup>* line, which  
210 was made by replacing a LacZ-carrying P-element insertion with a Gal4 element (P  
211 [Gal4,w+]) into the *bab<sup>P</sup>* site in the intronic region of *bab1* gene (CABRERA *et al.* 2002).  
212 The driver *bab:GAL4* (genotype: *w[\*]; P{bab1[Pgal<sup>4-2</sup>]/TM6B, Tb[1]}*) is expressed in all  
213 larval ovarian somatic cells (CABRERA *et al.* 2002; COUDERC *et al.* 2002; SARIKAYA *et al.*  
214 2012; SALER *et al.* 2020). We used this *bab:GAL4* transgenic line to express GFP in larval  
215 ovarian somatic cells, allowing us to separate the somatic tissue from the germ line tissue  
216 using Fluorescence-Activated Cell Sorting (FACS).

217 The expression of the gene *nanos* (*nos*) is limited to germ line cells in the larval  
218 ovary (WANG AND LIN 2004). We used a *nos:Gal4* transgenic line (genotype:  
219  $P\{w[+mC]=UAS-Dcr-2.D\}1, w[1118]; P\{w[+mC]=GAL4-nos.NGT\}40$ ) to express GFP  
220 exclusively in the germ line cells, and thus isolate the germ line cells using FACS (TRACEY  
221 *et al.* 2000).

222 We dissociated ovaries at the three stages described above and isolated the GFP-  
223 positive cells at each stage using FACS. Cellular debris was eliminated with gate R1, non-  
224 singlets were eliminated by gate R2, and the R3 gate selected for GFP positive cells. A  
225 combination of the three gates yielded singlet GFP positive cells, minimizing the  
226 possibility of tissue contamination by undissociated cells. When similar number of ovaries  
227 were used to obtain sorted cells for somatic and germ line tissue-types, we found larger  
228 number of somatic cells as compared to germ cells as expected, indicating a successful  
229 separation of the desired tissue type (**Supplementary Figure S2**).

230 With this method, we obtained tissue-specific transcriptomes of somatic and germ  
231 line tissues at the same three stages of terminal filament development used to generate  
232 the whole ovary dataset. We sequenced three biological replicates for all datasets and  
233 retained replicates that had at least 10 million reads. The number of reads aligned to the  
234 genome ranged from 11.0 to 81.5 million. Greater than 94.09% of reads aligned in all  
235 datasets, with the single exception of one dataset (Mid-1) with 88.55 % of aligned reads  
236 (**Supplementary Table S1, Supplementary Figure S3**). The PCA analysis based on the  
237 counts normalized by variance-stabilization transformation (VST) shows a clear  
238 separation of somatic and germ cell libraries along the first principal component,  
239 suggesting a successful separation of cell types by FACS (**Figure 3A**). For the somatic

240 samples, the three biological replicates cluster closely together (**Figure 3A-B**) while the  
241 different stages are separated from each other in the second principal component. The  
242 structure of the dendrogram for the somatic samples resembles that of the whole ovary,  
243 in which early and mid-stages are closer to each other than either is to the late stage. As  
244 for the germ cell libraries, unlike the biological replicates of the early and late stages, the  
245 mid-stage replicates do not cluster together. A possible explanation is the low number of  
246 reads from the sample Mid-1 (**Supplementary Table S1, Supplementary Figure S3**).

247 To further assess the successful separation of somatic and germ cells, we checked  
248 the expression of well-known tissue-type-specific markers. The genes *nanos* and *vasa*  
249 are two genes known to be specifically expressed in germ cells in the ovary (SCHUPBACH  
250 AND WIESCHAUS 1986; LEHMANN AND NUSSLEIN-VOLHARD 1991). Both genes show higher  
251 expression in the germ cell libraries than in the somatic cell libraries (mean  $\log_2(\text{Fold}$   
252  $\text{Change})$  of 8.37 for *nanos*, and 8.23 for *vasa*) (**Figure 3C**), confirming that the preparation  
253 and sequencing of the germ cell libraries successfully captured the germ cells and their  
254 RNAs, and suggesting that germ cells were not present (or present only at very low levels)  
255 in the somatic cell libraries. *bab1*, *bab2*, and *tj* are considered somatic gene markers  
256 (SAHUT-BARNOLA *et al.* 1995a; COUDERC *et al.* 2002). These three somatic markers display  
257 higher expression levels in our somatic libraries than in the germ cell libraries at each  
258 stage (mean  $\log_2(\text{Fold Change})$  -0.31 for *bab1*, -1.31 for *bab2*, and -1.70 for *tj*) (**Figure**  
259 **3D**). However, in four of the 18 libraries, either *bab1* or *bab2* (but not *tj*) showed higher  
260 expression levels in a specific germ cell library than in the somatic libraries. These specific  
261 cases were as follows: (1) one early stage germ cell replicate had higher *bab1* levels than  
262 one of the early somatic replicates; (2) two mid stage germ cell replicates had higher *bab1*

263 levels than the somatic replicates; (3) one late stage germ cell replicate had higher *bab1*  
264 levels than the somatic replicates; (4) one mid stage germ cell replicate had higher *bab2*  
265 levels than the somatic replicates. This could indicate that some somatic cells might have  
266 been included in these particular germ cell libraries. Nonetheless, despite this putative  
267 small amount of contamination, we can clearly differentiate both tissue types based on  
268 their expression profiles as shown in the PCA (**Figure 3A**), suggesting that we captured  
269 the transcriptional differences between cell types (**Figure 3A**) sufficiently to allow us to  
270 achieve our goal of successfully retrieving the genes that are highly and differentially  
271 expressed in each of these two tissues.

272

### 273 **Differential expression analysis of somatic and germ line tissues across all stages**

274 The differential expression analysis between the somatic and germ line tissues across all  
275 three stages revealed 1,880 genes significantly upregulated (adjusted p-value<0.01) in  
276 germ cells and 1,585 genes significantly upregulated in the somatic cells (**Figure 4A;**  
277 **Supplementary Table S4**).

278 Among the 20 most significant genes (with the lowest adjusted p-value)  
279 overexpressed in germ cells relative to somatic cells, we detected known germ line-  
280 specific genes including piRNA biogenesis genes *Argonaute3 (AGO3)*, *krimper (krimp)*,  
281 and *tejas (tej)*, along with *Aubergine (aub)*, (BRENNECKE *et al.* 2007; OLIVIERI *et al.* 2010;  
282 PATIL AND KAI 2010; SATO *et al.* 2015), *sisters unbound (sunn)* (KRISHNAN *et al.* 2014),  
283 *benign gonial cell neoplasm (bgcn)* (OHLSTEIN *et al.* 2000), and uncharacterized genes  
284 including *CG32814* and *CG12851* on the chromosome 2R. As for the somatic cells, the  
285 most significantly overexpressed gene relative to the germ cells is the cytochrome gene

286 *Cyp4p2*, whose role is unknown in the ovary, followed by cytochrome *Cyp4p1* and the  
287 uncharacterized genes CG32581 and CG42329. Some genes known to play roles in the  
288 ovary were also among this group, including the regulator of the niche cells and ecdysone  
289 receptor *Taiman (tai)* (KÖNIG *et al.* 2011), and the regulator of vitellogenesis *apterous (ap)*  
290 (GAVIN AND WILLIAMSON 1976).

### 291 **Temporally dynamic expression of genes previously studied in somatic ovary** 292 **development**

293 We explored the expression dynamics of some of the previously studied genes expressed  
294 in the *Drosophila* ovary. To our knowledge, temporal gene expression studies in the larval  
295 ovary for many these genes have not yet been conducted.

296 First, we considered the temporal expression patterns of some adhesion proteins  
297 known to play a role in ovary development. *RanBPM* is an adhesion linker protein  
298 expressed in the germ line niche in the adult ovary (DANSEREAU AND LASKO 2008). In our  
299 dataset we see opposing trends of expression levels in somatic and germ line tissues,  
300 such that in germ line tissue *RanBPM* expression decreases progressively from early to  
301 mid to late stages, while in the somatic tissue it increases from early to mid to late stages  
302 (**Supplementary Figure S4A**). Cofilin (encoded by the gene *twinstar*) is an adhesion  
303 protein required for terminal filament cell rearrangement during terminal filament  
304 morphogenesis, as well as for adult border cell migration (CHEN *et al.* 2001). Cofilin shows  
305 similar germ line and somatic cell expression trends, with higher levels at early stages  
306 that decrease progressively at mid and late stages (**Supplementary Figure S4B**).

307 We then looked at temporal expression of *RhoGEF64C* and *Wnt4*, genes involved  
308 in cell motility. *RhoGEF64C* is a small apically localized RhoGTPase that regulates cell

309 shape and migration in the ovary (SIMOES *et al.* 2006). In our datasets we found  
310 *RhoGEF64C* expressed at higher levels in early and late stage somatic cells than at mid  
311 stages (**Supplementary Figure S4C**). *Wnt4* is involved in cell motility during ovarian  
312 morphogenesis (COHEN *et al.* 2002) and is expressed in the posterior terminal filaments  
313 and other somatic cell types of the third instar larval ovary (SLAIDINA *et al.* 2020). We  
314 found *Wnt4* to be expressed in lower levels in early and middle stages while the  
315 expression increases significantly in the late stage (**Supplementary Figure S4D**).

316 We also examined the temporal expression dynamics of a number of terminal  
317 filament cell-type-specific genes previously identified in a single cell sequencing study of  
318 the late third larval instar ovary (SLAIDINA *et al.* 2020). For example, *Diuretic hormone 44*  
319 *receptor 2 (Dh442)* was identified as highly expressed in terminal filament cells (SLAIDINA  
320 *et al.* 2020). In our datasets, we observed a significant increase in expression levels only  
321 at the late stage relative to early and mid-stage expression levels (**Supplementary**  
322 **Figure S4E**). Additional genes known to function in terminal filaments are *engrailed*,  
323 *invected*, *hedgehog* and *patched* (FORBES *et al.* 1996; BESSE *et al.* 2005; BOLÍVAR *et al.*  
324 2006; SALER *et al.* 2020). In our datasets we observed *engrailed* and its paralog *invected*  
325 expressed at lowest levels at the early stage, showing a progressive increase in  
326 expression levels from mid to late stages (**Supplementary Figure S4 F-G**). Interestingly,  
327 *invected*, but not *engrailed*, showed significant differential expression between early and  
328 mid-stages. The genes *patched* and *hedgehog* also showed significant increase from  
329 early to mid-stage (**Supplementary Figure S4H-I**).

330 Finally, we considered members of the *Fibroblast Growth Factor (FGF)* signaling  
331 pathway, which controls sheath cell proliferation in the pupal ovary (IRIZARRY AND

332 STATHOPOULOS 2015). Three key genes of this pathway, the FGF ligand *thisbe*, the FGF  
333 scaffolding protein *stumps* and the upstream FGF signaling activator *heartless*, show  
334 significantly higher differential expression levels at early to mid-stage than at mid to late  
335 stages (**Supplementary Figure S4J-L**). These temporal profiles add to our  
336 understanding of the roles of these genes in ovarian morphogenesis by suggesting  
337 distinct putative critical regulatory periods for different genetic pathways.

338

### 339 **Functional enrichment analysis of differentially expressed genes in somatic and** 340 **germ line tissues across all stages**

341 To gain insight into the general functional categories of genes likely involved in ovarian  
342 germ cell and somatic behaviors during terminal filament development, we performed a  
343 gene ontology (GO) enrichment analysis of the biological processes of differentially  
344 expressed genes across cell types and developmental stages (ASHBURNER *et al.* 2000).  
345 We found 31 level four GO-terms enriched (adjusted p-value<0.05) within the upregulated  
346 genes in germ cells, and 188 level four GO-terms enriched in the upregulated genes in  
347 somatic cells (**Supplementary Figure S5**). This analysis highlighted clear differences in  
348 the biological functions performed by the genes expressed in each tissue. The GO-terms  
349 enriched in the germ cells are primarily related to meiotic processes (9/31 contain the  
350 words “meiosis” or “meiotic”), chromosome stability (6/31 contain the words  
351 “chromosome” or “karyosome”) and cell cycle (12/31 contain “cell cycle”). In contrast, the  
352 GO-terms enriched in the somatic cells are principally related to cellular response (21/188  
353 contain “response”), development (18/188), growth (16/188), morphogenesis (10/188)  
354 cell migration (6/188 contain the word “migration”) and signaling pathways (6/188).

355 To complement this GO enrichment analysis, we performed a KEGG pathway  
356 enrichment analysis on the same cell-type-specific overexpressed genes. The KEGG  
357 pathway database is a manually curated database of molecular interactions used to study  
358 enrichment of genetic regulatory pathways in gene lists (KANEHISA AND GOTO 2000). With  
359 this analysis, we identified nine KEGG pathways significantly enriched in the germ cells,  
360 and 16 significantly enriched pathways in the somatic cells (adjusted p-value<0.05)  
361 (**Figure 4B**). The KEGG pathways enriched in the germ cells are generally related to  
362 meiosis and genome protection, while upregulated genes in the somatic cells are  
363 enriched for pathways involved in cell proliferation and cell death, including the previously  
364 identified *Hippo* (BARRY AND CAMARGO 2013; SARIKAYA AND EXTAVOUR 2015; ZHENG AND  
365 PAN 2019) and *MAPK* (SHAUL AND SEGER 2007) signaling pathways.

366

### 367 **Stage- and tissue-specific differential gene expression analysis**

368 To explore the functions of the stage-specific upregulated genes in each tissue type, we  
369 performed a differential expression analysis of somatic versus germ tissue at each of the  
370 three stages (**Supplementary Figure S6; Supplementary Table S5**) and then  
371 performed a GO analysis of biological functions and KEGG pathway enrichment analysis  
372 on the six sets of differentially expressed genes (upregulated at early, mid, and late stages  
373 in germ and somatic cells). The GO enrichment analysis of the genes differentially  
374 expressed in somatic cells over time (**Supplementary Figure S6A-C**) revealed that four  
375 key biological processes are consistent throughout all three stages including the mid  
376 stage, which has the smallest number of differentially expressed genes across stages.  
377 Specifically, these are the GO terms taxis, cell growth, actin filament-based process and

378 cell adhesion. At early and late stages, we additionally observe many key biological  
379 processes related to morphogenesis in the somatic cells, including cell proliferation,  
380 differentiation and migration.

381 To obtain a finer-grained view of the dynamic regulation of ovary development  
382 during terminal filament formation, we also performed differential expression analysis and  
383 functional enrichment analysis of somatic and germ line tissue types at each of the three  
384 stages. In the somatic cells the number of differentially expressed genes between the  
385 early and mid-stages (867 genes) is lower than between the mid and late stages (1,404  
386 genes) (**Figure 5A; Supplementary Table S6**). To identify genes with stage-specific  
387 upregulation, we compared each stage to the other two stages. We identified a higher  
388 number of stage-specific upregulated genes in early (1,227) and late stages (1,409) than  
389 at mid (139) (**Figure 5B; Supplementary Table S7**).

390 The germ cells, in general, display fewer differentially expressed genes between  
391 stages than the somatic cells. From early to mid-stages there are twice as many  
392 differentially expressed genes (557 genes) as from mid to late stages (248 genes) (**Figure**  
393 **5C; Supplementary Table S8**). In terms of stage-specific upregulated genes, the highest  
394 number of such genes are found at early stages (209), followed by mid (186), and late  
395 (84) stages (**Figure 5D; Supplementary Table S9**). The 1,227, 139, and 1,409 genes  
396 found upregulated at early, mid, and late stages respectively of somatic tissue were  
397 enriched for two KEGG pathways at early stages, one at mid-stage and 17 in late stages  
398 (**Figure 5E**). This analysis allowed us to pinpoint the stage(s) at which specific pathways  
399 were enriched in somatic cells relative to germ cells, which included Apoptosis, *Hippo*  
400 signaling, and *MAPK* signaling. In addition, we detected some signaling pathways

401 enriched only in somatic cells at late stages, such as the *Hedgehog*, *FoxO*, and *Notch*  
402 pathways (**Figure 5E**).

403         Given the known role of the Hippo pathway in cell proliferation (Wu *et al.* 2003;  
404 HUANG *et al.* 2005; BARRY AND CAMARGO 2013), and specifically in terminal filament cell  
405 and terminal filament number regulation (SARIKAYA AND EXTAVOUR 2015), we proceeded  
406 to analyze the expression patterns of the genes belonging to the core Hippo signaling  
407 pathway. We found that most Hippo pathway core genes display increasing expression  
408 levels from early to mid to late stages, with the exception of the expression of the core  
409 gene *Rae1* which progressively decreases in expression level from early to late stages  
410 (**Supplementary Figure S7**).

411 In the germ cells, across stages we find fewer processes directly involved in development  
412 and morphogenesis with gene ontology categories belonging to meiosis and cell cycle  
413 (**Supplementary Figure S6**). Among the 209, 186, and 84 upregulated genes in germ  
414 cells at early, mid, and late stages respectively, only one KEGG pathway (Ribosome) and  
415 one biological process GO-term (cytoplasmic translation) were found significantly  
416 enriched at early-stages. No such enrichment was detected at mid-stages, and three  
417 KEGG pathways were enriched at late stages (**Supplementary Figure S8**).

#### 418 **Uncharacterized genes**

419 The detection of uncharacterized genes among the top differentially expressed genes in  
420 germ cells drove us to ask if there were any differences in the proportion of  
421 uncharacterized genes in each set of differentially expressed genes. We found that in the  
422 genes significantly upregulated in somatic cells compared to germ cells, 29.15% are  
423 categorized as “uncharacterized proteins” in FlyBase (LARKIN *et al.* 2021), while within the

424 significantly upregulated genes in germ cells, the proportion of uncharacterized genes  
425 was 39.10%. Within the stage-specific upregulated genes, the proportion of  
426 uncharacterized genes remained constant (between 28.96% and 29.63%) in somatic  
427 cells, while in germ cells it increased from 29.08% in early stages, to 34.83% in mid  
428 stages, and to 37.40% in late stages (**Supplementary Figure S9**).

429

### 430 **Expression of cell type-specific markers**

431 A previous single cell RNA-sequencing dataset of the late third stage larval ovary  
432 (SLAIDINA *et al.* 2020) identified transcriptional profile clusters interpreted as indicative of  
433 cell types, and suggested gene markers associated with each cell type. To determine  
434 whether the cell types identified at this late stage might also be present at earlier  
435 developmental stages than that previously assessed, we examined the expression levels  
436 of those suggested marker across our datasets. As expected, the majority of the germ  
437 cell markers are highly expressed in our germ cell libraries and expressed only at low  
438 levels in the somatic cells (**Supplementary Figure S10**). Among the somatic markers  
439 detected in our somatic tissue libraries, we do not observe any particular temporal  
440 expression pattern specific to a given somatic cell type. Nevertheless, we clearly  
441 distinguish two groups of somatic markers (**Supplementary Figure S11**). One group is  
442 composed of somatic markers whose expression levels are highest at early and mid-  
443 stages, and decay at the late stage, and a larger group of makers that are less strongly  
444 expressed at early stages, show increased expression at the mid stage, and show highest  
445 expression at late stages. By contrast, the germ cell markers detected in our germ cell  
446 libraries do not display any clear temporal expression pattern. Instead, most of these

447 genes were expressed at similar levels across the three studied stages (**Supplementary**  
448 **Figure S12**). This is consistent with our previous observations that the germ line dataset  
449 is not enriched for any signaling pathway directly implicated in development during these  
450 three times points as the somatic cells do (**Supplementary Figure S6**).

451

## 452 **DISCUSSION**

### 453 **Temporal gene expression during ovary morphogenesis**

454 We systematically staged and sequenced entire larval ovaries to generate a gene  
455 expression dataset during terminal filament formation. We then separated somatic and  
456 germ line tissues during these stages and generated tissue-specific transcriptomes. While  
457 the development of the *Drosophila* ovary has been studied for the last several decades,  
458 and progress has been made on identifying the roles of some signaling pathways in its  
459 morphogenesis (COHEN *et al.* 2002; BESSE *et al.* 2005; GILBOA AND LEHMANN 2006; GANCZ  
460 *et al.* 2011; GANCZ AND GILBOA 2013; MATSUOKA *et al.* 2013; GILBOA 2015; IRIZARRY AND  
461 STATHOPOULOS 2015; LENGIL *et al.* 2015; MENDES AND MIRTH 2016; PANCHAL *et al.* 2017)  
462 to our knowledge, there are no publicly available transcriptomes of larval ovaries of  
463 *Drosophila* across developmental time. Recent articles have reported single cell RNA-  
464 sequencing for *Drosophila* ovaries, focusing either on a single larval time point or on adult  
465 ovaries (JEVITT *et al.* 2020; RUST *et al.* 2020; SLAIDINA *et al.* 2020; SLAIDINA *et al.* 2021).  
466 Our stage and tissue-type specific data thus represent a valuable complementary  
467 transcriptomic resource on the morphogenesis of the larval ovaries of *Drosophila*, a  
468 complex process that ultimately influences reproductive capacity.

## 469 **Differential gene expression across developmental stages of the larval ovary**

470 Both the whole ovary datasets and the somatic tissue datasets show increased numbers  
471 of differentially expressed genes from the mid-to-late stage transition, and in the late  
472 stage of terminal filament formation in the larval ovary (**Figure 2D,5A**). In contrast, germ  
473 cells show higher numbers of differentially expressed genes in the early to-mid stage  
474 transition, and in the early stages. The similarity in differentially expressed gene numbers  
475 and signaling pathways in the whole ovary and somatic cell datasets suggests that  
476 because the somatic cells are higher in number than the germ cells (**Supplementary**  
477 **Figure S2**), their transcriptomes dominate the whole-ovary transcriptomes derived from  
478 late stages of larval ovary development. Further functional enrichment analyses of  
479 somatic and germ line tissue revealed that distinct functions and pathways likely operate  
480 in these two cell types during larval ovary development.

481 It is possible that germ cells may be especially sensitive to DNA damage given  
482 their role in propagating genetic material, which we speculate may explain the enrichment  
483 of processes related to nucleotide replication, recombination and repair in our analysis of  
484 the differentially expressed genes in germ cells (**Figures 4B, S5**). Similarly, we observed  
485 many genes of the piRNA pathway (e.g., *AGO3*, *aub*, *krimp*, *tej*), which protect the  
486 genome from transposable elements (**Supplementary Table S5**) (SATO AND SIOMI 2020)  
487 among the top significantly enriched genes in germ cells. On the other hand, the somatic  
488 tissue is enriched for different signaling pathways including Hippo, MAPK, and apoptosis  
489 (**Figures 5E, S6**), which are known to play a role in either larval or adult ovary  
490 morphogenesis (LYNCH *et al.* 2010; KHAMMARI *et al.* 2011; ELSHAER AND PIULACHS 2015;  
491 SARIKAYA AND EXTAVOUR 2015). The observation of a higher number of uncharacterized

492 genes in the germ line tissue datasets (**Supplementary Figure S9**) highlights the  
493 importance of future functional characterization of these genes to understand their  
494 possible roles in germ line gene regulation.

495

#### 496 **Cell adhesion and migration during ovary morphogenesis**

497 We assessed the temporal dynamics of genes expressed in specific cell types during  
498 development to serve as generators of new hypotheses to understand the role of genes  
499 and pathways during morphogenesis. *RhoGEF64C* is a RhoGTPase with some role in  
500 regulating control cell shape changes that lead to epithelial cell invagination (SIMOES *et al.*  
501 *al.* 2006; TORET AND LE BIVIC 2021). In a genome-wide association study on ovariole  
502 number phenotypes in natural populations of *Drosophila*, *RhoGEF64C* driven in somatic  
503 tissue had a significant effect on adult ovariole number (LOBELL *et al.* 2017). The  
504 significant increase in expression of *RhoGEF64C* we observed in early and late stages  
505 (**Figure S4C**) suggests its role in somatic cell shape and migration in both early and late  
506 stages.

507 GO-terms related to cell adhesion, motility and taxis were enriched in all three stages in  
508 somatic cells (**Supplementary Figure S6**). Previous studies have shown signaling  
509 pathways involved in ovary development to affect cell adhesion and migration processes  
510 (COHEN *et al.* 2002; LI *et al.* 2003; BESSE *et al.* 2005; LAI *et al.* 2017). Migratory events in  
511 mid to late stages of the larval ovary have been described for two ovarian cell types,  
512 swarm cells and sheath cells (SAHUT-BARNOLA *et al.* 1995a; SAHUT-BARNOLA *et al.* 1996;  
513 GREEN II AND EXTAVOUR 2012; SLAIDINA *et al.* 2020). The increased number of  
514 differentially expressed genes that correspond to the processes of cell migration and

515 adhesion may be due to the migratory events in the mid- to late stages of larval ovary  
516 morphogenesis.

517         The FGF signaling pathway supports terminal filament cell differentiation in the  
518 early larval stages through *thisbe (ths)* and upstream activator *heartless (htl)*, and also  
519 controls sheath cell proliferation in late larval and pupal stages (IRIZARRY AND  
520 STATHOPOULOS 2015). In our dataset, we observe that in somatic cells these FGF pathway  
521 genes show a significant progressive upregulation from early to mid and from mid to late  
522 stages (**Supplementary Figure S4J-L**). Consistently, *ths* and *stumps* were identified as  
523 markers of a distinct migratory ovarian cell population, the sheath cells (SLAIDINA *et al.*  
524 2020). The gene *stumps* is expressed in sheath cells in stages corresponding to our “late”  
525 stage in the differentiating terminal filament cells and in pupal stages (144h AEL), of  
526 migratory sheath cells (IRIZARRY AND STATHOPOULOS 2015).

527

## 528 **Functional enrichment analysis and signaling pathways**

529 Our results show that in the late stage of somatic cells there is an increase in expression  
530 of genes involved in multiple signaling pathways, including the Wnt, MAPK, Hippo,  
531 Hedgehog, FoxO, TGF and Notch pathways (**Figure 5E**). The molecular mechanisms of  
532 all these signaling pathways during larval ovary development have not yet been  
533 extensively studied, but all of them have been functionally implicated in ovariole number  
534 determination by a large-scale genetic screen (KUMAR *et al.* 2020).

535         We previously showed that Hippo signaling pathway controls proliferation of  
536 somatic cells, which affects terminal filament number (SARIKAYA AND EXTAVOUR 2015).

537 Our differential gene expression data show that members of the Hippo pathway are  
538 significantly differentially expressed in the somatic tissue (**Figure 4B; Supplementary**  
539 **Figure S8**). Loss of function mutations in Yki, an effector of the Hippo signaling pathway,  
540 cause increased growth and reduced apoptosis through an increase in the levels of the  
541 cell cycle protein Cyc E and the apoptosis inhibitor Diap1 (HARVEY *et al.* 2003; HUANG *et*  
542 *al.* 2005). In our somatic cell datasets, we observe *Diap1* transcript levels significantly  
543 increase from early to late stages, and those of *CycE* increase from mid to late stages  
544 (**Supplementary Figure S13A-B**). However, the Apoptosis KEGG pathway appears  
545 significantly enriched in the somatic late stage (**Figure 5E; Supplementary Figure S6**) .  
546 Furthermore, apoptosis-related genes *Dronc* and *Dark*, which form the apoptosome  
547 (**Supplementary Figure 13C, D**) (YUAN *et al.* 2011), are also significantly upregulated in  
548 the late stage, as are the caspases *Dcp-1*, *Drice*, and *Dredd* (**Supplementary Figure**  
549 **13C, E-G**) (HARVEY *et al.* 2001). Thus, we observe both an upregulation of apoptosis and  
550 an upregulation of the apoptosis inhibition genes in late stage somatic cells. This could  
551 mean that genes controlling apoptosis both positively and negatively are acting to exert  
552 tight control of this process. Alternatively, our observations may reflect that each process  
553 is upregulated within different somatic cell types.

554 Cap cells and intermingled cells are somatic cells that interact with the germ cells  
555 for the maintenance of germ line stem cell niches (LI *et al.* 2003; SONG *et al.* 2007). The  
556 Notch signaling pathway, enriched in the late-stage somatic dataset (**Figure 5E;**  
557 **Supplementary Figure S6C**), is required for cap cell fate (PANCHAL *et al.* 2017; YATSENKO  
558 AND SHCHERBATA 2021). We observed an expression level increase in Notch pathway  
559 components at late stages, suggesting that the role of the Notch pathway in cap cell fate

560 determination may be particularly important at mid to late stages of larval ovary  
561 development.

562 Components of the TGF $\beta$  pathway, enriched in late stage somatic cells in our  
563 dataset (**Figure 5C**), are known to contribute to ovarian development. These include the  
564 Bone Morphogenetic Protein (BMP) and Activin pathways of the TGF $\beta$  pathway (PANGAS  
565 AND WOODRUFF 2000; GUO AND WANG 2009). The BMP ligand *decapentaplegic* (*dpp*) was  
566 previously documented as expressed in all larval ovarian somatic cells and in cap cells of  
567 late third instar larval ovary (XIE AND SPRADLING 1998; SATO *et al.* 2010; SALER *et al.* 2020).  
568 The expression of *dpp* in the larval ovary is dependent on the expression of *bab* genes  
569 (SALER *et al.* 2020). The activin pathway, controls terminal filament cell proliferation and  
570 differentiation (LENGIL *et al.* 2015). We find that the activin receptor *baboon* shows a  
571 significant expression level increase in the late stage somatic cells (adjusted p-value of  
572 0.002602) and could indicate its role in terminal filament cell differentiation in late stage.

573

## 574 **Conclusions**

575 Here we provide a dataset that explores gene expression during larval ovary development  
576 and morphogenesis, which is crucial to understand how the ovary is shaped in early  
577 stages to develop into a functional adult organ. This work offers a dataset for the  
578 developmental biology community to probe the genetic regulation of larval ovarian  
579 morphogenesis.

580

## 581 **MATERIALS AND METHODS**

## 582 **Fly Stocks**

583 Flies were reared at 25°C at 60% humidity with food containing yeast and in uncrowded  
584 conditions. The following two fly lines were obtained from the Bloomington *Drosophila*  
585 Stock Center:  $w[*]; P\{bab1[Pgal^{4-2}]/TM6B, Tb[1]$  (abbreviated herein as *bab:GAL4*; stock  
586 number 6803),  $P\{w[+mC]=UAS-Dcr-2.D\}1, w[1118]; P\{w[+mC]=GAL4-nos.NGT\}40$   
587 (abbreviated herein as *nos:GAL4*; stock number 25751).  $w[1118], P[UAS\ Stinger]$   
588 (abbreviated herein as *UAS: Green Stinger I*, (BAROLO *et al.* 2000) used for GFP  
589 expression was a gift from Dr. James Posakony (University of California, San Diego).  
590 Crosses were set with 100-200 virgin UAS females and 50-100 GAL4 males in a 180 ml  
591 bottle containing 50ml standard fly media one day prior to egg laying.

592

## 593 **Staging larvae**

594 To obtain uniformly staged larvae for the experiments, a protocol was devised to collect  
595 eggs that were near-synchronously laid, from which the larvae were then collected. To  
596 obtain a desired genotype, crosses were set as described above. The cross was set at  
597 25°C at 60% humidity and left overnight to mate. Hourly egg collections were set up on  
598 60 mm apple juice-agar plates (9 g agar, 10 g sugar, 100 ml apple juice and 300 ml water)  
599 with a pea-sized spread of fresh yeast paste (baker's yeast granules made into a paste  
600 in a drop of tap water). Eggs were collected hourly for eight hours. The first two collection  
601 plates were discarded to remove asynchronously laid eggs that may have been retained  
602 inside the females following fertilization. Staged first instar larvae were collected into vials  
603 24 hours after egg collection. Larvae at 72h AEL (hours After Egg Laying) were  
604 designated as early stage, at 96h AEL as middle stage and at 120h AEL as late stage of

605 Terminal Filament development. For a step-by-step detailed protocol see  
606 **Supplementary File 1.**

607

### 608 **Dissection and dissociation of larval ovary**

609 Staged larvae were collected for dissection every hour. The head of the larva was  
610 removed with forceps and the cuticle and gut were carefully pulled with one forceps while  
611 holding the fat body with another forceps. This process left just the fat bodies in the  
612 dissection dish as long as the larvae were well fed and fattened with yeast. Ovaries  
613 located in the center of the length of each fat body were then dissected free of the fat  
614 body using an insulin syringe needle (BD 328418). Ovaries dissected clear of fat body  
615 were collected in DPBS (Thermo Fisher 14190144) and batches of 20-30 ovaries in DPBS  
616 were kept on ice until dissociation. Ovaries were harvested hourly at the appropriate  
617 times, placed on ice immediately following dissection, and maintained on ice for a  
618 maximum of four hours before dissociation and subsequent FACS processing.

619 Dissociation of the larval ovary required two enzymatic steps. After seven hours of  
620 dissection, batches of dissected ovaries were placed in 0.25% Trypsin solution (Thermo  
621 Fisher 25200056) for ten minutes at room temperature in the cavity of a glass spot plate  
622 (Fisher Scientific 13-748B). They were then transferred to another cavity containing 2.5  
623 % Liberase (5 g Liberase reconstituted in 2ml nuclease free water; Sigma 5401119001)  
624 and teased apart with insulin syringe needles until most of the clumps were separated  
625 and left (without agitation) at room temperature for ten minutes. Using a 200µl pipette with  
626 a filter tip (pre rinsed in 1X PBS), the dissociated cells in Liberase were pipetted up and  
627 down gently ten times to uniformly mix and separate the cells. The cell suspension was

628 then transferred to an RNA Lobind tube (Eppendorf 8077-230) and placed on a vortexer  
629 for 1 minute. Meanwhile the well was rinsed in 1.4 ml of PBS by pipetting repeatedly. This  
630 PBS was then mixed with the cell-suspension in Liberase and vortexed for another  
631 minute, and the entire sample was then placed on ice. This sample was then taken directly  
632 to the FACS facility on ice along with an RNA Lobind collection tube containing 100-200µl  
633 Trizol (Thermo Fisher 15596026). For a step-by-step detailed protocol see  
634 **Supplementary File 1.**

635

### 636 **Flow Sorting GFP-positive cells**

637 The dissociated tissue sample was sorted in a MoFlo Astrios EQ Cell sorter (Beckman  
638 Coulter) run with Summit v6.3.1 software. The dissociated cell solution was diluted and a  
639 flow rate of 200 events per second was maintained with high sorting efficiency (< 98%)  
640 during the sorting process. A scatter gate (R1) was employed to eliminate debris  
641 (**Supplementary Figure S2**) and a doublet gate (R2) was used to exclude non-singlet  
642 cells. A 488 nm emission Laser was used to excite the GFP, and the collection was at  
643 576 nm. The GFP-positive cells were designated in gate R3 and sorted directly into Trizol.  
644 The resulting cells collected in Trizol were frozen immediately by plunging the tube in  
645 liquid nitrogen and then stored at -80°C until RNA extraction. A single replicate consisted  
646 of at least 1000 cell counts pooled from FACS runs.

647

### 648 **RNA extraction**

649 Flow-sorted cells were stored at -80°C were thawed at room temperature. Trizol contents  
650 were lysed with a motorized pellet pestle (Kimble 749540-0000). Zymo RNA Micro-Prep  
651 kit (Zymo Research R2060) was used to isolate RNA from the Trizol preparations. Equal  
652 amounts of molecular grade ethanol (Sigma E7023) were added to Trizol and mixed well  
653 with a pellet pestle, then pipetted onto a spin column. All centrifugation steps were done  
654 at 10,000g for one minute at room temperature. The column was washed with 400µl Zymo  
655 RNA wash buffer and then treated with Zymo DNase (6U/µl) for 15 minutes at room  
656 temperature. The column was then washed twice with 400µl Zymo RNA Pre-wash buffer  
657 and once with Zymo RNA wash-buffer. The RNA was eluted from the column in 55 µl of  
658 Nuclease-free water (Thermo Fisher 10977015). The RNA obtained was quantified first  
659 using a NanoDrop (Model ND1000) spectrophotometer and then using a high sensitivity  
660 kit (Thermo Fisher Q32852) on a Qubit 3.0 Fluorometer (Thermo Fisher Q33216). It was  
661 also checked for integrity on a high sensitivity tape (Agilent 5067-5579) with an electronic  
662 ladder on an Agilent Tapestation 2200 or 4200. RNA extraction from staged whole ovaries  
663 was carried out by crushing entire ovaries in Trizol and following the same protocol  
664 described above. For a step-by-step detailed protocol see **Supplementary File 1**.

665

## 666 **Library Preparation**

667 cDNA libraries were prepared using the Takara Apollo library preparation kit (catalogue  
668 # 640096). Extracted RNA samples were checked for quality using Tapestation tapes.  
669 50µl of RNA samples were pipetted into Axygen PCR 8-strip tubes (Fisher Scientific 14-  
670 222-252) and processed through PrepX protocols on the Apollo liquid handling system.  
671 mRNA was isolated using PrepX PolyA-8 protocol (Takara 640098). The mRNA samples

672 were then processed for cDNA preparation using PrepX mRNA-8 (Takara 640096)  
673 protocol. cDNA products were then amplified for 15 cycles of PCR using longAmp Taq  
674 (NEB M0287S). During amplification PrepX RNAseq index barcode primers were added  
675 for each library to enable multiplexing. The amplified library was then cleaned up using  
676 PrepX PCR cleanup-8 protocol with magnetic beads (Aline C-1003). The final cDNA  
677 libraries were quantified using a high sensitivity dsDNA kit (Thermo Fisher Q32854) on a  
678 Qubit 3.0 Fluorometer (Thermo Fisher Q33216). cDNA content and quality were  
679 assessed with D1000 (Agilent 5067-5582) or High sensitivity D1000 tape (Agilent 5067-  
680 5584, when cDNA was in low amounts) on an Agilent TapeStation 2200 or 4200. For a  
681 step-by-step detailed protocol see **Supplementary File 1**.

682

### 683 **Sequencing cDNA libraries**

684 Libraries were sequenced on an Illumina HiSeq 2500 sequencer. Single end-50bp reads  
685 were sequenced on a high-throughput flow cell. Libraries of varying concentrations were  
686 normalized to be equimolar, the concentrations of which ranged between 2-10nM per  
687 lane. All the samples in a flow cell were multiplexed and later separated based on unique  
688 prepX indices to yield at least 10 million reads per library. The reads were demultiplexed  
689 and trimmed of adapters using the bcl2fastq2 v2.2 pipeline to yield final fastq data files.

690

### 691 **RNA-seq data processing**

692 The *D. melanogaster* genome assembly and gene annotations were obtained from  
693 FlyBase version dmel\_r6.36\_FB2020\_05 (LARKIN *et al.* 2021). The reads were aligned

694 with RSEM v1.3.3 (LI AND DEWEY 2011) and using STAR v2.7.6a as read aligner (DOBIN  
695 *et al.* 2013) we obtained the gene counts in each library. Because some of the tissue-  
696 specific biological samples were sequenced in more than one lane or run, and therefore  
697 the reads were split into multiple fastq files, the gene counts belonging to the same  
698 biological sample were summed. Gene counts in each dataset were normalized with the  
699 variance stabilizing transformation (VST) method implemented in the DESeq2 v1.26.0  
700 (LOVE *et al.* 2014) R package. Further analyses, such as principal component analysis,  
701 hierarchical clustering, and differential expression analysis, were performed in R using  
702 the VST-normalized counts.

703

#### 704 **Differential Expression (DE) analysis**

705 The differential expression analyses were performed with DESeq2 v1.26.0 (LOVE *et al.*  
706 2014). On the whole ovary dataset, the contrasts tested were early vs mid, and mid vs  
707 late stages. For the tissue-specific datasets, three different comparisons were performed.  
708 First, to identify differentially expressed genes independently of the stage, all stages of  
709 somatic cells were compared to all stages of germ cells. Second, to identify genes up-  
710 regulated in a stage-specific manner within each tissue, we compared the expression  
711 level at each stage to the mean expression level of the other two stages. Third, we  
712 compared germ cells and somatic cells independently at each stage. Genes with a  
713 Benjamini-Hochberg (BH) adjusted p-value lower than 0.01 were selected as differentially  
714 expressed in the corresponding contrast.

715

## 716 **Functional analysis**

717 The Gene Ontology (GO) and Kyoto Encyclopedia of Genes and Genomes (KEGG)  
718 pathways enrichment analyses were performed on the differentially expressed genes with  
719 the `enrichGO` and `enrichKEGG` functions of the `clusterProfiler` package (v3.14.3) for R  
720 (Yu *et al.* 2012). The GO terms were obtained using the R package `AnnotationDbi`  
721 (CARLSON 2015) with the database `org.Dm.eg.db` v3.10.0. The GO overrepresentation  
722 analysis of biological process (BP) was performed against the gene universe of all *D.*  
723 *melanogaster* annotated genes in `org.Dm.eg.db`, adjusting the p-values with the  
724 Benjamini-Hochberg method (BH), adjusted p-value and q-value cutoff of 0.01, and a  
725 minimum of 30 genes per term. For the KEGG enrichment analysis, p-values were  
726 adjusted by the BH procedure, and an adjusted p-value cutoff of 0.05 was used.

727

## 728 **Data availability**

729 All the raw data are publicly available at NCBI-Gene Expression Omnibus (GEO)  
730 database under the accession code GSE172015. The scripts used to process and  
731 analyze the data are available at GitHub repository  
732 [https://github.com/guillemylla/Ovariole\\_morphogenesis\\_RNAseq](https://github.com/guillemylla/Ovariole_morphogenesis_RNAseq).

733

## 734 **Competing Interests**

735 The authors have no competing interests to declare.

736

737 **Acknowledgements**

738 This study was supported by National Institutes of Health NICHD award R01-HD073499-  
739 01 to CGE, funds from Harvard University, and the Google Cloud Academic Research  
740 Credits Program. We thank the flow cytometry and genomics staff at the Bauer Core  
741 Facility of Harvard University Faculty of Arts and Sciences (FAS) for advice on FACS  
742 sorting and sequencing, the FAS Research Computing group for advice on initial data  
743 analysis, and Extavour lab members for discussion.

744 **FIGURE LEGENDS**

745

746 **Figure 1: Experimental scheme for generating stage-specific transcriptomes of**  
747 **germ cells and somatic cells of larval ovaries during terminal filament formation.**

748 **A)** Location of the larval ovaries (white circles within the larva), and illustration of larval  
749 ovary development divided into three stages during terminal filament formation (colored  
750 in black). **B)** Left to right: location of the ovaries in an adult female abdomen; a single  
751 adult ovary containing multiple ovarioles; an individual ovariole; anterior tip of an ovariole  
752 enlarged to show the germarium and terminal filament (black) at the tip. **C)**  
753 Representation of the three stages of whole larval ovaries from the wild type strain Oregon  
754 R, chosen for library preparation and sequencing (light gray: early stage, gray: mid, dark  
755 gray: late). **D)** Somatic cells and **E)** germ cells from developing ovaries at the three chosen  
756 stages were labelled with GFP using tissue specific GAL4 lines (somatic cells in shades  
757 of cyan and germ cells in shades of magenta). Somatic cells were labelled using  
758 *bab:GAL4* (genotype: *w[\*]; P{w[+mW.hs]=GawB}bab1[Pgal4-2]/TM6B, Tb[1]*) and germ  
759 cells were labeled using *nos:GAL4* (genotype: *P{w[+mC]=UAS-Dcr-2.D}1, w[1118];*  
760 *P{w[+mC]=GAL4-nos.NGT}40*) and **F)** GFP-positive cells were separated using FACS.  
761 **G)** Schematics of representative plot layouts of somatic and germ line tissue separation  
762 using FACS. Y axis: autofluorescence, 488-576/21 Height Log; X axis: GFP fluorescence  
763 intensity, 488-513/26 Height Log (see Supplementary Figure S2 for actual representative  
764 data plots). **H)** Separated cells or whole ovaries were processed for mRNA extraction and  
765 cDNA library preparation followed by high throughput sequencing. h AEL = hours After  
766 Egg Laying.

767 **Figure 2: Whole ovary RNA-seq dataset overview. A)** hierarchical clustering  
768 dendrogram and **B)** PCA of the whole ovary RNA-seq dataset, both showing that  
769 biological replicates are similar to each other, and that early and mid-stages are more  
770 similar to each other than either of them is to late stage. **C)** Number of differentially  
771 expressed genes between early and mid stages, and between mid and late stages  
772 (adjusted p-value<0.01; black: upregulated genes; white: downregulated genes). See  
773 Supplementary Table S2 for gene list. **D)** Number of significantly upregulated stage-  
774 specific genes (adjusted p-value<0.01). See Supplementary Table S3 for gene list. **E)**  
775 Heatmap showing the expression of all the stage-specific upregulated genes as a row-  
776 wise z-score. Genes are clustered hierarchically and separated into three groups using  
777 the function “cutree”, and grayscale row labels (“\*Gene DE”) immediately to the right of  
778 the tree are colored based on the stage in which the gene was detected to be significantly  
779 upregulated (x axis categories).

780

781 **Figure 3: Cell type-specific RNA-seq dataset concordance and positive controls. A)**  
782 **PCA Plot and B)** hierarchical clustering dendrogram of germ cell and somatic cell RNA-  
783 seq libraries. Expression in normalized counts by variance stabilization transformation  
784 (VST) in each of the cell-type-specific RNA-seq libraries of **C)** known germ cell markers  
785 *nanos* and *vasa*, and **D)** known somatic cell markers *bric a brac 1*, *bric a brac 2*, and  
786 *traffic jam*.

787

788 **Figure 4: Transcriptomic differences between germ cells and somatic cells. A)**  
789 Number of significantly upregulated genes (adjusted p-value<0.01) in germ cells and  
790 somatic cells. See Supplementary Table S4 for gene list. **B)** Significantly enriched KEGG  
791 pathways (adjusted p-value<0.05) within the upregulated genes of each cell type. The  
792 circle size is proportional to the number of differentially expressed genes that the  
793 indicated KEGG pathway contains, and the color gradient indicates the p-value.

794

795 **Figure 5: Cell type-specific differential expression analysis. A)** Number of  
796 differentially expressed genes (adjusted p-value<0.01) upregulated (black) and  
797 downregulated (white) in somatic cells between early and mid, and between mid and late  
798 stages. See Supplementary Table S6 for gene list. **B)** Number of differentially expressed  
799 genes (adjusted p-value<0.01) upregulated (black) and downregulated (white) in somatic  
800 cells at each stage compared to the two other stages. See Supplementary Table S7 for  
801 gene list. **C)** Number of differentially expressed genes (adjusted p-value<0.01)  
802 upregulated (black) and downregulated (white) in germ cells between early and mid, and  
803 between mid and late stages. See Supplementary Table S8 for gene list. **D)** Number of  
804 differentially expressed genes (adjusted p-value<0.01) upregulated (black) and  
805 downregulated (white) in germ cells at each stage compared to the two other stages. See  
806 Supplementary Table S9 for gene list. **E)** Significantly enriched (adjusted p-value<0.05)  
807 KEGG pathways within the upregulated genes at each somatic stage. Circle size is  
808 proportional to the number of differentially expressed genes it contains, and the color  
809 gradient indicates the p-value.

810 REFERENCES

- 811 Ashburner, M., C. A. Ball, J. A. Blake, D. Botstein, H. Butler *et al.*, 2000 Gene ontology:  
812 tool for the unification of biology. The Gene Ontology Consortium. *Nature Genetics*  
813 25: 25-29.
- 814 Ashburner, M., K. G. Golic and R. S. Hawley, 2005 *Drosophila: A Laboratory Handbook*.  
815 Cold Spring Harbor Laboratory Press, Cold Spring Harbor, NY.
- 816 Barolo, S., L. A. Carver and J. W. Posakony, 2000 GFP and beta-galactosidase  
817 transformation vectors for promoter/enhancer analysis in *Drosophila*.  
818 *Biotechniques* 29: 726, 728, 730, 732.
- 819 Barry, E. R., and F. D. Camargo, 2013 The Hippo superhighway: signaling crossroads  
820 converging on the Hippo/Yap pathway in stem cells and development. *Current*  
821 *Opinion in Cell Biology* 25: 247-253.
- 822 Besse, F., D. Busson and A. M. Pret, 2005 Hedgehog signaling controls Soma-Germen  
823 interactions during *Drosophila* ovarian morphogenesis. *Dev Dyn* 234: 422-431.
- 824 Bolivar, J., J. Pearson, L. Lopez-Onieva and A. Gonzalez-Reyes, 2006 Genetic dissection  
825 of a stem cell niche: the case of the *Drosophila* ovary. *Dev Dyn* 235: 2969-2979.
- 826 Bolívar, J., J. Pearson, L. López-Onieva and A. González-Reyes, 2006 Genetic dissection  
827 of a stem cell niche: the case of the *Drosophila* ovary. *Developmental Dynamics*  
828 235: 2969-2979.
- 829 Brand, A. H., and N. Perrimon, 1993 Targeted gene expression as a means of altering  
830 cell fates and generating dominant phenotypes. *Development* 118: 401-415.
- 831 Brennecke, J., A. A. Aravin, A. Stark, M. Dus, M. Kellis *et al.*, 2007 Discrete small RNA-  
832 generating loci as master regulators of transposon activity in *Drosophila*. *Cell* 128:  
833 1089-1103.
- 834 Büning, J., 1994 *The Insect Ovary: ultrastructure, previtellogenic growth and evolution*.  
835 Chapman and Hall, London.
- 836 Cabrera, G. R., D. Godt, P. Y. Fang, J. L. Couderc and F. A. Laski, 2002 Expression  
837 pattern of Gal4 enhancer trap insertions into the bric a brac locus generated by P  
838 element replacement. *Genesis* 34: 62-65.
- 839 Carlson, M., 2015 AnnotationDbi: Introduction To Bioconductor Annotation Packages.
- 840 Chen, J., D. Godt, K. Gunsalus, I. Kiss, M. Goldberg *et al.*, 2001 Cofilin/ADF is required  
841 for cell motility during *Drosophila* ovary development and oogenesis. *Nat Cell Biol*  
842 3: 204-209.
- 843 Church, S. H., B. A. S. de Medeiros, S. Donoughe, N. L. Marquez Reyes and C. G.  
844 Extavour, 2021 Repeated loss of variation in insect ovary morphology highlights  
845 the role of developmental constraint in life-history evolution. *Proceedings of the*  
846 *Royal Society of London. Series B: Biological Sciences* in press.
- 847 Cohen, E. D., M. C. Mariol, R. M. Wallace, J. Weyers, Y. G. Kamberov *et al.*, 2002 DWnt4  
848 regulates cell movement and focal adhesion kinase during *Drosophila* ovarian  
849 morphogenesis. *Dev Cell* 2: 437-448.
- 850 Couderc, J. L., D. Godt, S. Zollman, J. Chen, M. Li *et al.*, 2002 The bric a brac locus  
851 consists of two paralogous genes encoding BTB/POZ domain proteins and acts as  
852 a homeotic and morphogenetic regulator of imaginal development in *Drosophila*.  
853 *Development* 129: 2419-2433.

854 Dansereau, D. A., and P. Lasko, 2008 RanBPM regulates cell shape, arrangement, and  
855 capacity of the female germline stem cell niche in *Drosophila melanogaster*. *J Cell*  
856 *Biol* 182: 963-977.

857 David, J., 1970 Le nombre d'ovarioles chez la *Drosophila*: relation avec la fecondite et  
858 valeur adaptive [Number of ovarioles in *Drosophila melanogaster*: relationship with  
859 fertility and adaptive value]. *Arch. Zool. Exp. Gen* 111: 357-370.

860 Dobin, A., C. A. Davis, F. Schlesinger, J. Drenkow, C. Zaleski *et al.*, 2013 STAR: ultrafast  
861 universal RNA-seq aligner., pp. 15-21 in *Bioinformatics*.

862 Elshaer, N., and M. D. Piulachs, 2015 Crosstalk of EGFR signalling with Notch and Hippo  
863 pathways to regulate cell specification, migration and proliferation in cockroach  
864 panoistic ovaries. *Biol Cell* 107: 273-285.

865 Forbes, A. J., H. Lin, P. W. Ingham and A. C. Spradling, 1996 hedgehog is required for  
866 the proliferation and specification of ovarian somatic cells prior to egg chamber  
867 formation in *Drosophila*. *Development* 122: 1125-1135.

868 Gancz, D., and L. Gilboa, 2013 Insulin and Target of rapamycin signaling orchestrate the  
869 development of ovarian niche-stem cell units in *Drosophila*. *Development* 140:  
870 4145-4154.

871 Gancz, D., T. Lengil and L. Gilboa, 2011 Coordinated regulation of niche and stem cell  
872 precursors by hormonal signaling. *PLoS Biology* 9: e1001202.

873 Gavin, J. A., and J. H. Williamson, 1976 Juvenile hormone-induced vitellogenesis in  
874 *Apterous4*, a non-vitellogenic mutant in *Drosophila melanogaster*. *Journal of Insect*  
875 *Physiology* 22: 1737-1742.

876 Gilboa, L., 2015 Organizing stem cell units in the *Drosophila* ovary. *Current Opinion in*  
877 *Genetics & Development* 32C: 31-36.

878 Gilboa, L., and R. Lehmann, 2004 Repression of primordial germ cell differentiation  
879 parallels germ line stem cell maintenance. *Curr Biol* 14: 981-986.

880 Gilboa, L., and R. Lehmann, 2006 Soma-germline interactions coordinate homeostasis  
881 and growth in the *Drosophila* gonad. *Nature* 443: 97-100.

882 Godt, D., and F. A. Laski, 1995a Mechanisms of cell rearrangement and cell recruitment  
883 in *Drosophila* ovary morphogenesis and the requirement of *bric a brac*.  
884 *Development* 121: 173-187.

885 Godt, D., and F. A. Laski, 1995b Mechanisms of cell rearrangement and cell recruitment  
886 in *Drosophila* ovary morphogenesis and the requirement of *bric à brac*.  
887 *Development* 121: 173-187.

888 Green, D. A., 2nd, and C. G. Extavour, 2014 Insulin signalling underlies both plasticity  
889 and divergence of a reproductive trait in *Drosophila*. *Proc Biol Sci* 281: 20132673.

890 Green II, D. A., and C. G. Extavour, 2012 Convergent Evolution of a Reproductive Trait  
891 Through Distinct Developmental Mechanisms in *Drosophila*. *Developmental*  
892 *Biology* 372: 120-130.

893 Guo, X., and X. F. Wang, 2009 Signaling cross-talk between TGF-beta/BMP and other  
894 pathways. *Cell Res* 19: 71-88.

895 Harvey, K. F., C. M. Pfleger and I. K. Hariharan, 2003 The *Drosophila* Mst ortholog, hippo,  
896 restricts growth and cell proliferation and promotes apoptosis. *Cell* 114: 457-467.

897 Harvey, N. L., T. Daish, K. Mills, L. Dorstyn, L. M. Quinn *et al.*, 2001 Characterization of  
898 the *Drosophila* caspase, DAMM. *J Biol Chem* 276: 25342-25350.

- 899 Hodin, J., 2009 Chapter 11: She Shapes Events As They Come: Plasticity in Female  
900 Insect Reproduction, pp. 423-521 in *Phenotypic Plasticity of Insects*, edited by D.  
901 Whitman and T. N. Ananthkrishnan. Science Publishers, Inc., Enfield, NH.
- 902 Hodin, J., and L. M. Riddiford, 2000a Different mechanisms underlie phenotypic plasticity  
903 and interspecific variation for a reproductive character in drosophilids (Insecta:  
904 Diptera). *Evolution* 54: 1638-1653.
- 905 Hodin, J., and L. M. Riddiford, 2000b Different mechanisms underlie phenotypic plasticity  
906 and interspecific variation for a reproductive character in Drosophilids (Insecta:  
907 Diptera). *Evolution* 5: 1638-1653.
- 908 Honek, A., 1993 Intraspecific Variation in Body Size and Fecundity in Insects - a General  
909 Relationship. *Oikos* 66: 483-492.
- 910 Huang, J., S. Wu, J. Barrera, K. Matthews and D. Pan, 2005 The Hippo signaling pathway  
911 coordinately regulates cell proliferation and apoptosis by inactivating Yorkie, the  
912 *Drosophila* Homolog of YAP. *Cell* 122: 421-434.
- 913 Irizarry, J., and A. Stathopoulos, 2015 FGF signaling supports *Drosophila* fertility by  
914 regulating development of ovarian muscle tissues. *Dev Biol* 404: 1-13.
- 915 Jevitt, A., D. Chatterjee, G. Xie, X. F. Wang, T. Otwell *et al.*, 2020 A single-cell atlas of  
916 adult *Drosophila* ovary identifies transcriptional programs and somatic cell lineage  
917 regulating oogenesis. *PLoS Biol* 18: e3000538.
- 918 Kanehisa, M., and S. Goto, 2000 KEGG: kyoto encyclopedia of genes and genomes.  
919 *Nucleic Acids Res* 28: 27-30.
- 920 Khammari, A., F. Agnes, P. Gandille and A. M. Pret, 2011 Physiological apoptosis of polar  
921 cells during *Drosophila* oogenesis is mediated by Hid-dependent regulation of  
922 Diap1. *Cell Death Differ* 18: 793-805.
- 923 King, R. C., 1970 *Ovarian development in Drosophila melanogaster*. Academic Press.
- 924 King, R. C., S. K. Aggarwal and U. Aggarwal, 1968 The Development of the Female  
925 *Drosophila* Reproductive System. *Journal of Morphology* 124: 143-166.
- 926 König, A., A. S. Yatsenko, M. Weiss and H. R. Shcherbata, 2011 Ecdysteroids  
927 affect *Drosophila* ovarian stem cell niche formation and early germline  
928 differentiation. *The EMBO Journal* 30: 1549-1562.
- 929 Krishnan, B., S. E. Thomas, R. Yan, H. Yamada, I. B. Zhulin *et al.*, 2014 Sisters Unbound  
930 Is Required for Meiotic Centromeric Cohesion in *Drosophila melanogaster*.  
931 *Genetics* 198: 947-965.
- 932 Kumar, T., L. Blondel and C. G. Extavour, 2020 Topology-driven analysis of protein-  
933 protein interaction networks detects functional genetic sub-networks regulating  
934 reproductive capacity. *eLife* 9: e54082.
- 935 Lai, C. M., K. Y. Lin, S. H. Kao, Y. N. Chen, F. Huang *et al.*, 2017 Hedgehog signaling  
936 establishes precursors for germline stem cell niches by regulating cell adhesion.  
937 *Journal of Cell Biology* 216: 1439-1453.
- 938 Larkin, A., S. J. Marygold, G. Antonazzo, H. Attrill, G. Dos Santos *et al.*, 2021 FlyBase:  
939 updates to the *Drosophila melanogaster* knowledge base. *Nucleic Acids Res* 49:  
940 D899-D907.
- 941 Leatherman, J. L., and T. A. Jongens, 2003 Transcriptional silencing and translational  
942 control: key features of early germline development. *Bioessays* 25: 326-335.

943 Lehmann, R., and C. Nusslein-Volhard, 1991 The maternal gene nanos has a central role  
944 in posterior pattern formation of the *Drosophila* embryo. *Development* 112: 679-  
945 691.

946 Lengil, T., D. Gancz and L. Gilboa, 2015 Activin signaling balances proliferation and  
947 differentiation of ovarian niche precursors and enables adjustment of niche  
948 numbers. *Development* 142: 883-892.

949 Li, B., and C. N. Dewey, 2011 RSEM: accurate transcript quantification from RNA-Seq  
950 data with or without a reference genome., pp. 323 in *BMC Bioinformatics*.

951 Li, M., X. Hu, S. Zhang, M. S. Ho, G. Wu *et al.*, 2019 Traffic jam regulates the function of  
952 the ovarian germline stem cell progeny differentiation niche during pre-adult stage  
953 in *Drosophila*. *Sci Rep* 9: 10124.

954 Li, M. A., J. D. Alls, R. M. Avancini, K. Koo and D. Godt, 2003 The large Maf factor Traffic  
955 Jam controls gonad morphogenesis in *Drosophila*. *Nature Cell Biology* 5: 994-  
956 1000.

957 Lobell, A. S., R. R. Kaspari, Y. L. Serrano Negron and S. T. Harbison, 2017 The Genetic  
958 Architecture of Ovariolo Number in *Drosophila melanogaster*: Genes with Major,  
959 Quantitative, and Pleiotropic Effects. *G3 (Bethesda)* 7: 2391-2403.

960 Love, M. I., W. Huber and S. Anders, 2014 Moderated estimation of fold change and  
961 dispersion for RNA-seq data with DESeq2. *Genome Biol* 15: 550.

962 Lynch, J. A., A. D. Peel, A. Drechsler, M. Averof and S. Roth, 2010 EGF signaling and  
963 the origin of axial polarity among the insects. *Curr Biol* 20: 1042-1047.

964 Markow, T. A., and P. M. O'Grady, 2007 *Drosophila* biology in the genomic age. *Genetics*  
965 177: 1269-1276.

966 Matsuoka, S., Y. Hiromi and M. Asaoka, 2013 Egfr signaling controls the size of the stem  
967 cell precursor pool in the *Drosophila* ovary. *Mech Dev* 130: 241-253.

968 Mendes, C. C., and C. K. Mirth, 2016 Stage-Specific Plasticity in Ovary Size Is Regulated  
969 by Insulin/Insulin-Like Growth Factor and Ecdysone Signaling in *Drosophila*.  
970 *Genetics* 202: 703-719.

971 Ohlstein, B., C. A. Lavoie, O. Vef, E. Gateff and D. M. McKearin, 2000 The *Drosophila*  
972 cystoblast differentiation factor, benign gonial cell neoplasm, is related to DExH-  
973 box proteins and interacts genetically with bag-of-marbles. *Genetics* 155: 1809-  
974 1819.

975 Olivieri, D., M. M. Sykora, R. Sachidanandam, K. Mechtler and J. Brennecke, 2010 An in  
976 vivo RNAi assay identifies major genetic and cellular requirements for primary  
977 piRNA biogenesis in *Drosophila*. *EMBO J* 29: 3301-3317.

978 Panchal, T., X. Chen, E. Alchits, Y. Oh, J. Poon *et al.*, 2017 Specification and spatial  
979 arrangement of cells in the germline stem cell niche of the *Drosophila* ovary  
980 depend on the Maf transcription factor Traffic jam. *PLoS Genet* 13: e1006790.

981 Pangas, S. A., and T. K. Woodruff, 2000 Activin signal transduction pathways. *Trends*  
982 *Endocrinol Metab* 11: 309-314.

983 Patil, V. S., and T. Kai, 2010 Repression of Retroelements in *Drosophila* Germline via  
984 piRNA Pathway by the Tudor Domain Protein Tejas. *Current Biology* 20: 724-730.

985 Rust, K., L. E. Byrnes, K. S. Yu, J. S. Park, J. B. Sneddon *et al.*, 2020 A single-cell atlas  
986 and lineage analysis of the adult *Drosophila* ovary. *Nat Commun* 11: 5628.

987 Sahut-Barnola, I., B. Dastugue and J.-L. Couderc, 1996 Terminal filament cell  
988 organization in the larval ovary of *Drosophila melanogaster*. ultrastructural

989 observations and pattern of divisions. Roux's Archives of Developmental Biology  
990 205: 356-363.

991 Sahut-Barnola, I., D. Godt, F. A. Laski and J.-L. Couderc, 1995a *Drosophila* Ovary  
992 Morphogenesis: Analysis of Terminal Filament Formation and Identification of a  
993 Gene Required for This Process. *Developmental Biology* 170: 127-135.

994 Sahut-Barnola, I., D. Godt, F. A. Laski and J. L. Couderc, 1995b *Drosophila* ovary  
995 morphogenesis: analysis of terminal filament formation and identification of a gene  
996 required for this process. *Dev Biol* 170: 127-135.

997 Saler, L. M., M., V. Hauser, M. Bartoletti, C. Mallart, M. Malartre *et al.*, 2020 The Bric-à-  
998 Brac BTB/POZ transcription factors are necessary in niche cells for germline stem  
999 cells establishment and homeostasis through control of BMP/DPP signaling in the  
1000 *Drosophila melanogaster* ovary. *PLOS Genetics* 16: e1009128.

1001 Sarikaya, D. P., A. A. Belay, A. Ahuja, A. Dorta, D. A. Green, 2nd *et al.*, 2012 The roles  
1002 of cell size and cell number in determining ovariole number in *Drosophila*. *Dev Biol*  
1003 363: 279-289.

1004 Sarikaya, D. P., and C. G. Extavour, 2015 The Hippo pathway regulates homeostatic  
1005 growth of stem cell niche precursors in the *Drosophila* ovary. *PLoS Genetics* 11:  
1006 e1004962.

1007 Sato, K., and M. C. Siomi, 2020 The piRNA pathway in *Drosophila* ovarian germ and  
1008 somatic cells. *Proc Jpn Acad Ser B Phys Biol Sci* 96: 32-42.

1009 Sato, K., Yuka, A. Shibuya, P. Carninci, Y. Tsuchizawa *et al.*, 2015 Krimper Enforces an  
1010 Antisense Bias on piRNA Pools by Binding AGO3 in the *Drosophila* Germline.  
1011 *Molecular Cell* 59: 553-563.

1012 Sato, T., J. Ogata and Y. Niki, 2010 BMP and Hh signaling affects primordial germ cell  
1013 division in *Drosophila*. *Zoolog Sci* 27: 804-810.

1014 Schupbach, T., and E. Wieschaus, 1986 Maternal-effect mutations altering the anterior-  
1015 posterior pattern of the *Drosophila* embryo. *Roux's Arch Dev Biol* 195: 302-317.

1016 Shaul, Y. D., and R. Seger, 2007 The MEK/ERK cascade: from signaling specificity to  
1017 diverse functions. *Biochimica et Biophysica Acta* 1773: 1213-1226.

1018 Simoes, S., B. Denholm, D. Azevedo, S. Sotillos, P. Martin *et al.*, 2006  
1019 Compartmentalisation of Rho regulators directs cell invagination during tissue  
1020 morphogenesis. *Development* 133: 4257-4267.

1021 Slaidina, M., T. U. Banisch, S. Gupta and R. Lehmann, 2020 A single-cell atlas of the  
1022 developing *Drosophila* ovary identifies follicle stem cell progenitors. *Genes Dev*  
1023 34: 239-249.

1024 Slaidina, M., S. Gupta, T. Banisch and R. Lehmann, 2021 A single cell atlas reveals  
1025 unanticipated cell type complexity in *Drosophila* ovaries. *bioRxiv*: 427703.

1026 Song, X., G. B. Call, D. Kirilly and T. Xie, 2007 Notch signaling controls germline stem  
1027 cell niche formation in the *Drosophila* ovary. *Development* 134: 1071-1080.

1028 Toret, C. P., and A. Le Bivic, 2021 A potential Rho GEF and Rac GAP for coupled Rac  
1029 and Rho cycles during mesenchymal-to-epithelial-like transitions. *Small GTPases*  
1030 12: 13-19.

1031 Tracey, W. D., Jr., X. Ning, M. Klingler, S. G. Kramer and J. P. Gergen, 2000 Quantitative  
1032 analysis of gene function in the *Drosophila* embryo. *Genetics* 154: 273-284.

1033 Twombly, V., R. K. Blackman, H. Jin, J. M. Graff, R. W. Padgett *et al.*, 1996 The TGF-  
1034 beta signaling pathway is essential for *Drosophila* oogenesis. *Development* 122:  
1035 1555-1565.

1036 Wang, Z., and H. Lin, 2004 Nanos maintains germline stem cell self-renewal by  
1037 preventing differentiation. *Science* 303: 2016-2019.

1038 Wu, S., J. Huang, J. Dong and D. Pan, 2003 hippo encodes a Ste-20 family protein kinase  
1039 that restricts cell proliferation and promotes apoptosis in conjunction with salvador  
1040 and warts. *Cell* 114: 445-456.

1041 Xie, T., and A. C. Spradling, 1998 decapentaplegic is essential for the maintenance and  
1042 division of germline stem cells in the *Drosophila* ovary. *Cell* 94: 251-260.

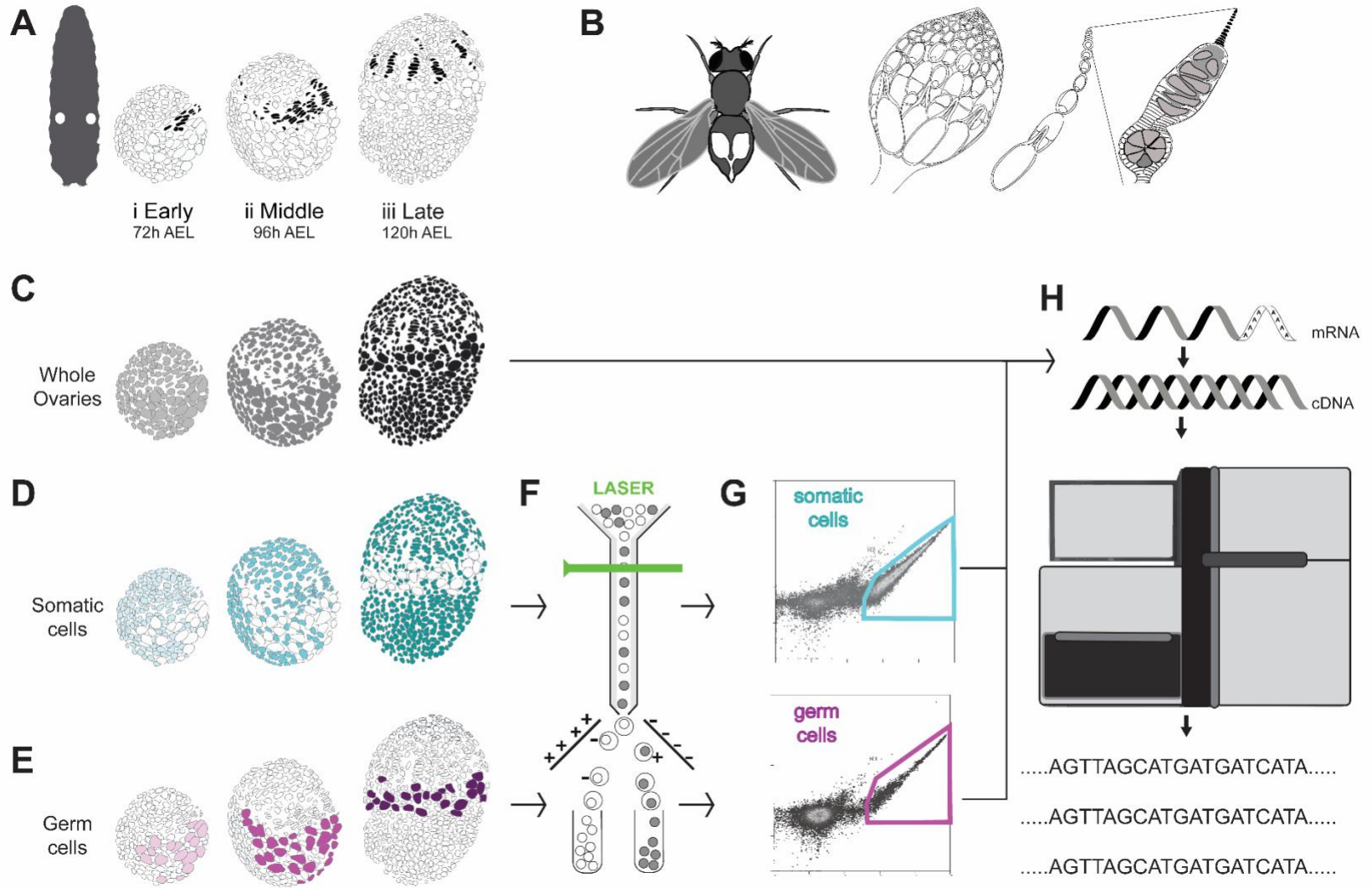
1043 Yatsenko, A. S., and H. R. Shcherbata, 2021 Distant activation of Notch signaling induces  
1044 stem cell niche assembly. *PLoS Genet* 17: e1009489.

1045 Yu, G., L. G. Wang, Y. Han and Q. Y. He, 2012 clusterProfiler: an R package for  
1046 comparing biological themes among gene clusters. *OMICS* 16: 284-287.

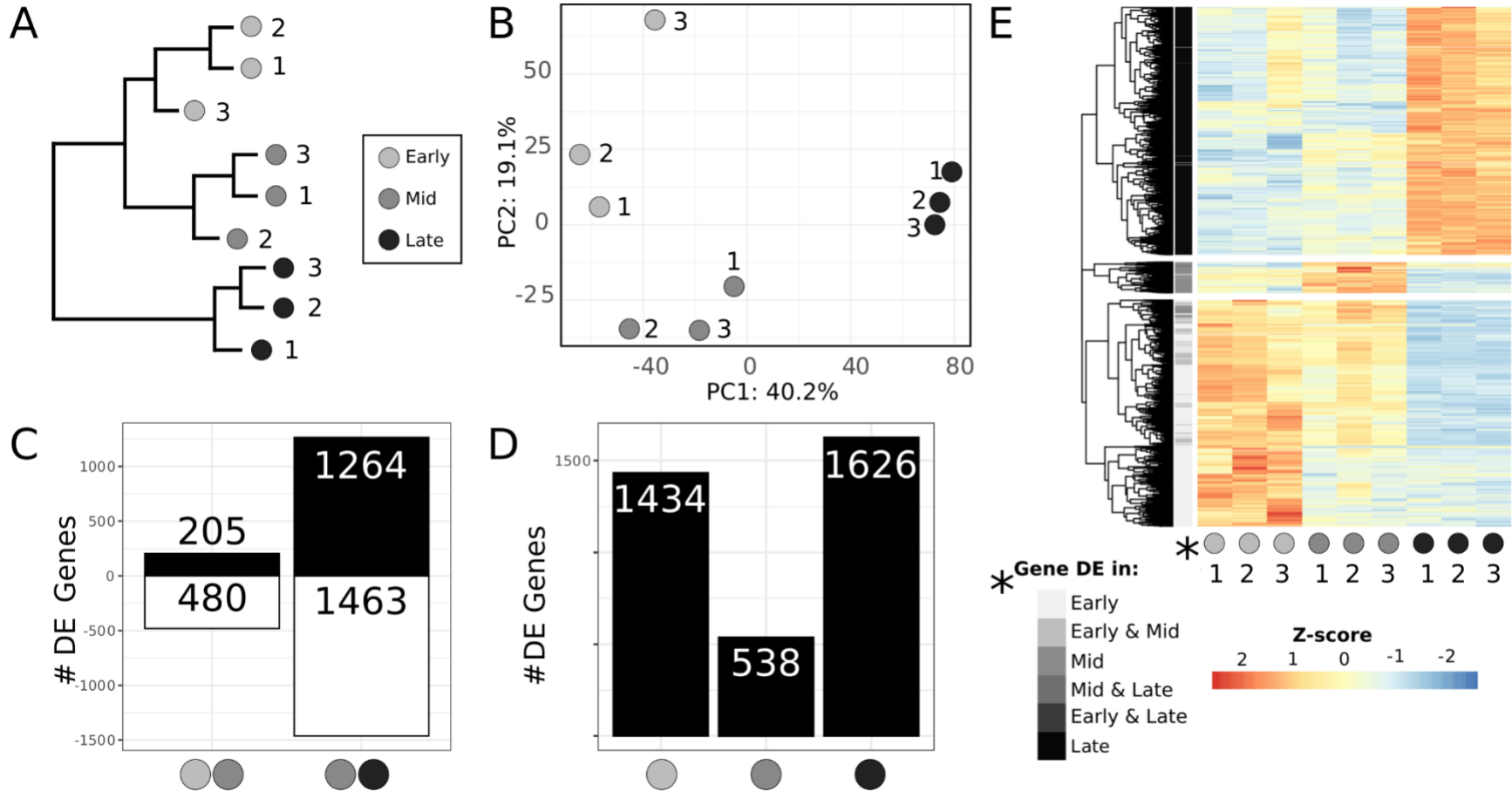
1047 Yuan, S., X. Yu, M. Topf, L. Dorstyn, S. Kumar *et al.*, 2011 Structure of the *Drosophila*  
1048 apoptosome at 6.9 Å resolution. *Structure* 19: 128-140.

1049 Zheng, Y., and D. Pan, 2019 The Hippo Signaling Pathway in Development and Disease.  
1050 *Dev Cell* 50: 264-282.

1051

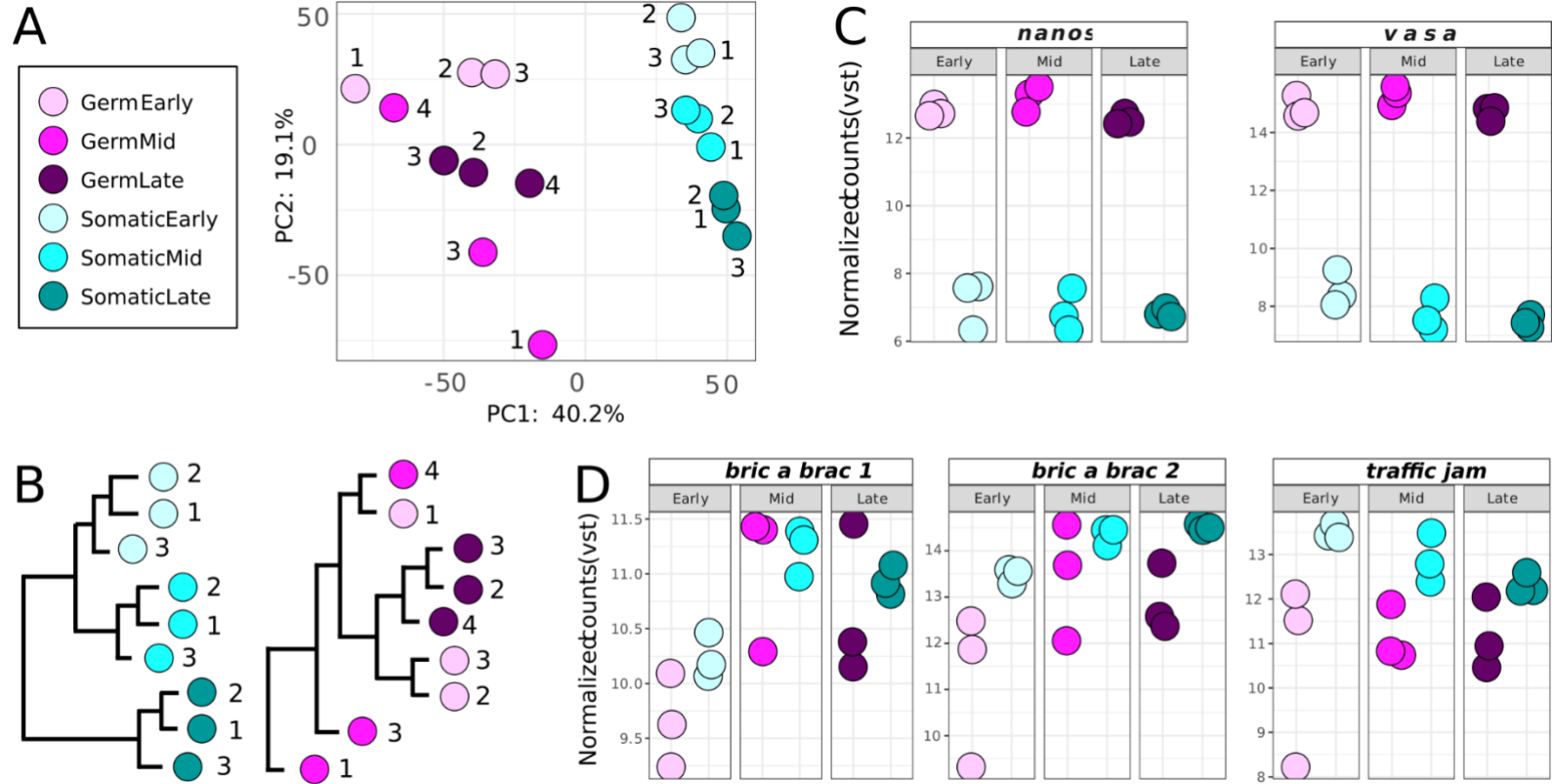


1054 **Figure 2**

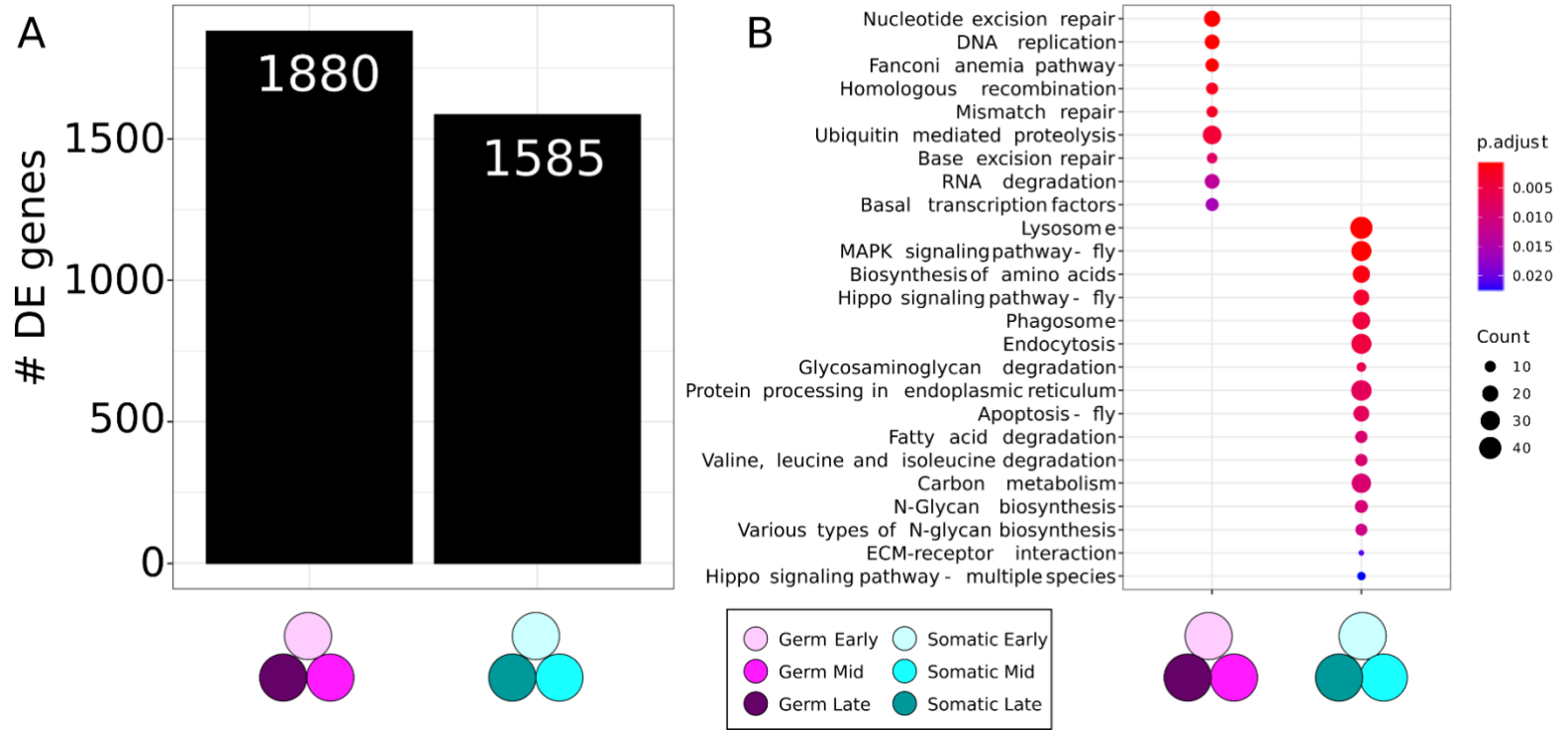


1055

1056

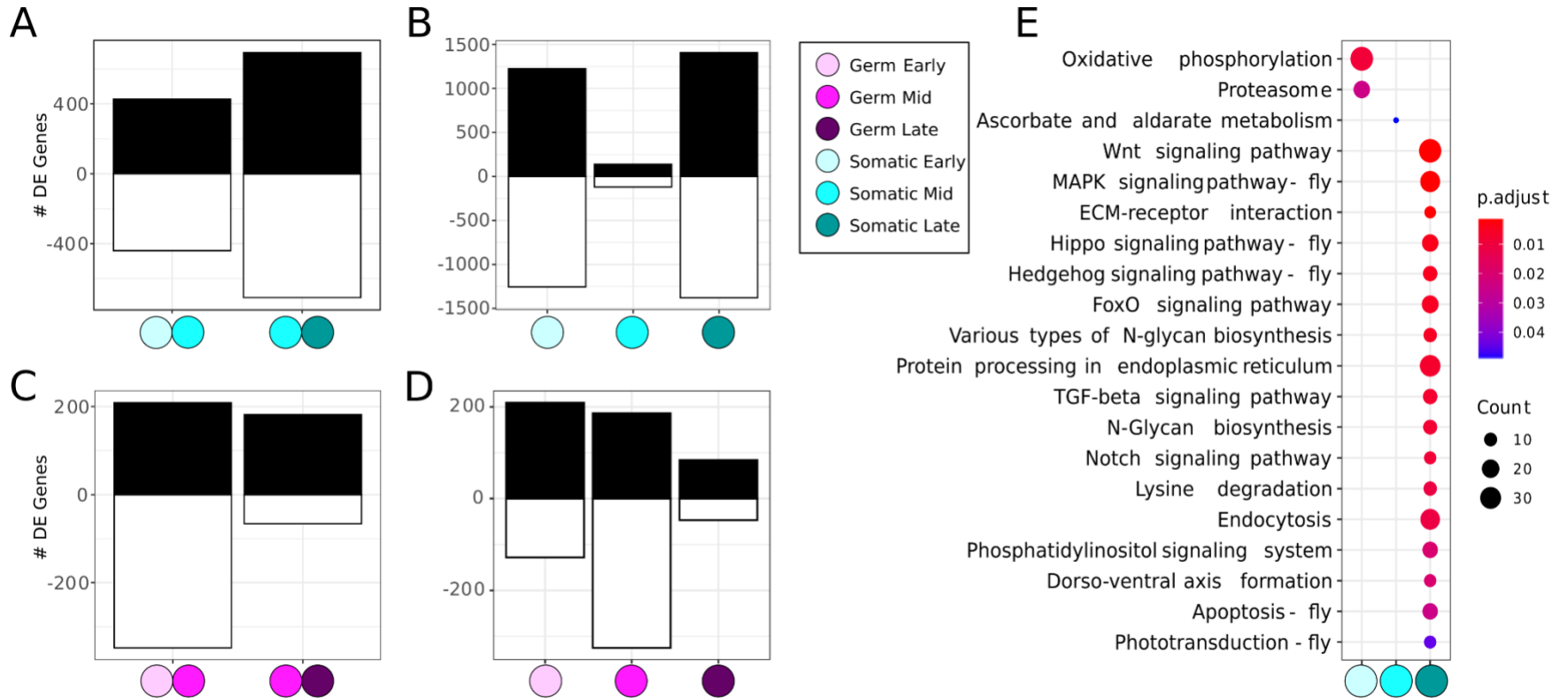


1059 **Figure 4**



1060

1061 **Figure 5**



1062

1063

1 **SUPPLEMENTARY MATERIALS (File S1)**

2  
3 **Distinct gene expression dynamics in germ line and somatic tissue during ovariole**  
4 **morphogenesis in *Drosophila melanogaster***

5  
6 *Shreeharsha Tarikere, Guillem Ylla and Cassandra G. Extavour*  
7

8  
9 These Supplementary Materials contain the following:

- 10
- 11 • Detailed Protocols
    - 12 I. Detailed protocol for staging larvae
    - 13 II. Detailed protocol for dissection and dissociation of larval ovaries
    - 14 III. Detailed RNA extraction protocol
    - 15 IV. Detailed library preparation protocol
  - 16 • Key Resources Table
  - 17 • Supplementary References
  - 18 • Legends for Supplementary Tables S1 through S9 (this document)
  - 19 • Supplementary Tables are provided in Supplementary Table files S1 through S9
  - 20 • Supplementary Figures S1 through S13 with Legends (this document)
- 21  
22

## 23 DETAILED PROTOCOLS

### 24 I. Detailed Protocol to stage larvae

- 25 1. Day 1: Collect 100 virgin females on the day before egg collection. Set the cross  
26 in a 50 ml media bottle with 50 males and leave at room temperature for 12h  
27 (overnight) to mate.
- 28 2. Make apple juice plates as follows:
  - 29 i. Boil 9g bacterial agar (Becton Dickinson catalog # 214050) in 300ml  
30 autoclaved distilled water.
  - 31 ii. Separately, dissolve and boil 10g Sucrose in 100ml apple juice.
  - 32 iii. Mix the two solutions together while stirring with a magnetic stir bar.
  - 33 iv. Pour the media into 60x15mm plates once the temperature has cooled  
34 down to approximately 50°C.
  - 35 v. Cool plates without lids for two hours and then cover with lids and store  
36 inverted at 4°C.
  - 37 vi. These plates can be used for up to two weeks.
- 38 3. Day 2: Remove apple juice agar plates needed for each hour for up to eight  
39 hours and allow them to warm up to room temperature.
- 40 4. In a glass vial, place some yeast granules and add tap water to cover the  
41 granules. There must be a drop of water more than the yeast granules can soak  
42 up. This makes a paste of peanut butter consistency.
- 43 5. Using a steel spatula, smear a pea-sized amount of paste onto one end of a  
44 plate, for all the plates. Optimize this based on the number of flies such that the  
45 paste is neither completely consumed nor remains in excess after an hour-long  
46 collection.
- 47 6. Transfer the cross in the bottle to a 100 ml collection cage and cover it  
48 immediately with an apple juice egg-collection plate containing yeast smear.  
49 Fasten the setup with two rubber bands.
- 50 7. Incubate with the plate at the bottom for one hour at 25°C. All activity from this  
51 point until the point of dissection is done at 25°C. For the first hourly change, tap  
52 the bottom of the cage and quickly replace the old plate with a fresh collection  
53 plate.
- 54 8. Remove any flies stuck to the yeast patch with forceps, crush and discard them  
55 in the freezer.
- 56 9. After the final egg plate flip transfer the flies back into a bottle using a funnel.  
57 Discard the first two collection plates. Incubate all the remaining plates at 25°C.
- 58 10. Day 3: Start collecting larvae at the end of the second hour egg collection done  
59 the previous day. Collect uniformly sized larvae.
- 60 11. Transfer around 50 larvae from the same staged egg collection into a vial. Some  
61 yeast paste may be carried to the vial during this collection; try to keep this  
62 amount constant.
- 63 12. Collect until the final hour of the previous days' collection. Incubate the vials  
64 containing larvae at 25°C.

## 67 II. Detailed protocol for dissection and dissociation of larval ovaries

- 68
- 69 1. Begin dissections at the same time as that of the third plate from the egg
- 70 collection day. Early-stage dissections take place three days from egg laying
- 71 (72h AEL), middle (mid) stage four days from egg laying (96h AEL), and larval
- 72 pupal stage (late) five days from egg laying (120h AEL).
- 73 2. Late stages are the easiest stage to locate and dissect, recognizable once the
- 74 late third instar larvae have immobilized on the side of the vial and have a
- 75 thickened cuticle. Use a fine wet paintbrush to dislodge them and place into cold
- 76 1x phosphate-buffered saline (PBS).
- 77 3. For early and middle stages, scrape the soggy layer of food from the vial using a
- 78 spatula and spread it on a glass petri dish. Under a dissecting stereomicroscope
- 79 select uniformly sized larvae, wash them in 1xPBS and place them into a fresh
- 80 glass dish with 1xPBS.
- 81 4. Male larvae are easily identified by the two translucent spots that are the testes
- 82 located at approximately 75% the length of the larval body from the anterior, and
- 83 by their relatively smaller body size compared to females. Adjusting the light
- 84 sources to be closer to the stage at the base of the glass dish allows better
- 85 visualization of ovaries and testes. Discard the males by using forceps to transfer
- 86 them onto a paper towel or kimwipe.
- 87 5. Using forceps, decapitate the larva. Gently squeeze out the inner contents from
- 88 posterior to anterior using forceps.
- 89 6. Pull the larval body away gently with forceps from the fat-body/gut, while holding
- 90 the body with another forceps. If done properly (after some experience) the larval
- 91 body and the gut material separate from the fat body lobes. Well-fed and later
- 92 stages of larvae are easier to dissect than younger stages.
- 93 7. The ovaries are located in the middle of the larval fat bodies. Ovaries are in a
- 94 flower-like circular patch in the center of the fat body. They are around 100-500
- 95  $\mu\text{m}$  in size depending on the stage, and appear as transparent tiny dots (early) to
- 96 large dots (pupal) within the fat body.
- 97 8. Using two insulin needles, hold the fat body close to the ovary with one needle
- 98 and use the other needle to cut closely around the ovary until it is released.
- 99 Some areas of the fat body may remain initially, which will be removed later
- 100 when the dissected ovaries are treated with trypsin.
- 101 9. Record the number of ovaries acquired in each batch.
- 102 10. Start to thaw an aliquot of liberase (stored at  $-20^{\circ}\text{C}$ ) to room temperature.
- 103 11. Dissect approximately 20 ovaries in this way, then place the glass dish on ice.
- 104 Use a fresh dish for the next round of dissections.
- 105 12. Use a 12-well glass plate and add 200 $\mu\text{l}$  of trypsin to one well and the contents of
- 106 the thawed liberase aliquot ( $\sim 150\mu\text{l}$ ) to the next well.
- 107 13. Clear any debris that surrounds the collected ovaries into a separate glass dish
- 108 using a needle. Using a 2 $\mu\text{l}$  pipette filter tip pre-rinsed in trypsin solution, transfer
- 109 the dissected ovaries into the trypsin well.
- 110 14. After transferring the last batch of ovaries into trypsin solution, incubate for 10
- 111 minutes in trypsin solution. Meanwhile label two RNA lobind tubes (Eppendorf
- 112 8077-230), with a black waterproof marker indicating the genotype of the

- 113 dissection, the date and the number of ovaries. Add the desired amount (100-  
114 200µl) of Trizol (based on the anticipated number of cells after sorting) to one of  
115 the two tubes (tube #1) – this tube will be used to collect cells following FACS  
116 (step 18). Leave the second tube (tube #2) empty – this will be used to collect the  
117 dissociated cells following enzymatic treatment (step 17). Place both tubes on  
118 ice.
- 119 15. Using a 2µl filter tip pre-rinsed in liberase solution, transfer the ovaries from  
120 trypsin into liberase. Dissociate them using needles until no clusters of cells can  
121 be seen. Incubate them in liberase solution for ten minutes, starting the clock  
122 when the ovaries are transferred from trypsin (includes time needed to dissociate  
123 using needles).
- 124 16. Place 200ml of liquid nitrogen in a liquid nitrogen container.
- 125 17. Using a 200µl pipette filter tip pre-rinsed in 1xPBS, pipette the tissue in liberase  
126 up and down gently ten times to dissociate and resuspend the cells. Transfer the  
127 contents to tube #2 and place it on a microtube vortexer for one minute.  
128 Meanwhile rinse the well that contained liberase with 1.4 ml of 1xPBS and pipette  
129 up and down 10 times. Add this volume into the tube and vortex for an additional  
130 10 minutes.
- 131 18. Place the tube on ice, remove one glove (so you can safely touch door handles)  
132 and carry the tube on ice, and your liquid nitrogen container, to your FACS  
133 facility/machine.
- 134 19. Collect cells following FACS into the Trizol in tube #1.
- 135

136 **III. Detailed RNA extraction protocol**

- 137
- 138 1. Because RNA extraction from FACS-sorted samples involves precious samples,
- 139 take care to work in an RNase-free environment. Wear lab coat, gloves and
- 140 safety goggles while working with Trizol and handling RNA samples.
- 141 2. Clean the table, ice bucket, pipettes, centrifuge, pellet pestle motor, table top
- 142 vortexer and tabletop mini-vortex first with 70% ethanol and then with RNase zap
- 143 (Thermo Fisher AM9780) on tissue paper.
- 144 3. Pellet pestles are cleaned first in 100% ethanol and then in nuclease free water
- 145 (Thermo Fisher 10977015). Prior to use the pestles should be sterilized in a
- 146 glass beaker covered in aluminum foil by autoclaving in a liquid cycle for 30 min.
- 147 4. Add 500  $\mu$ l Trizol into a lo-bind tube, which will be used to pre-rinse the pellet
- 148 pestle before crushing each sample.
- 149 5. Thaw Trizol cell samples (retrieved in tube #1 at step 19 in Protocol II) at room
- 150 temperature (RT) and place them on ice. Spin in tabletop mini-vortex for 10
- 151 seconds.
- 152 6. Crush each cell sample with a separate pellet pestle pre-rinsed in the Trizol set
- 153 aside for this purpose in step 4.
- 154 7. Crush cells in Trizol with a pre-rinsed pellet pestle. Add an equal volume of
- 155 100% ethanol, mix with pestle and vortex briefly. Spin samples briefly in tabletop
- 156 mini-vortex.
- 157 8. Pipette the sample onto a zymo spin column.
- 158 9. Wash column in 400  $\mu$ l RNA wash buffer. Centrifuge at 10,000 g for 1 minute at
- 159 RT.
- 160 10. Thaw DNase (Zymo kit: 6unit/ $\mu$ l) from storage at -20°C. Mix 5  $\mu$ l DNase with 35
- 161  $\mu$ l DNase digestion buffer per sample. Add 40  $\mu$ l of DNase mix to each column.
- 162 11. Incubate at RT for 15 minutes. Centrifuge at 10,000 g for 1 minute at RT..
- 163 12. Add 400  $\mu$ l RNA pre-wash buffer to the column and centrifuge. Repeat this step
- 164 one more time.
- 165 13. Add 700  $\mu$ l of RNA wash buffer. Centrifuge twice to completely remove the buffer
- 166 from the column, each time at 10,000 g for 1 minute at RT..
- 167 14. The column-bound RNA is eluted in two steps using nuclease-free water. Add 25
- 168  $\mu$ l water and incubate for 15 minutes at RT. Centrifuge at 10,000 g for 1 minute at
- 169 RT. Add another 20  $\mu$ l of water to elute a second time.
- 170 15. The library preparation protocol below (**IV**) requires RNA in a 50  $\mu$ l volume; an
- 171 additional 5  $\mu$ l is reserved for quality control measurements.
- 172 16. Quantify RNA first in Nanodrop RNA-40 measurement with 1.5  $\mu$ l of the sample.
- 173 Then use Qubit high sensitivity RNA kit to quantify 1 $\mu$ l of the sample (10 $\mu$ l
- 174 Standard1/2+190 Buffer/Reagent, 1  $\mu$ l sample+199 Buffer/Reagent).
- 175 17. Use a high-sensitivity RNA tape to quantify and measure the RNA integrity (RIN)
- 176 in a Tapestation. Use the standard protocol for high-sensitivity RNA quantification
- 177 using an electronic ladder for estimation of size.
- 178
- 179

#### 180 **IV. Detailed library preparation protocol (Takara Apollo system)**

181  
182 This is the Wafergen/Takara protocol. Low-throughput protocols process a maximum of  
183 eight samples at a time in the Apollo liquid handling unit. Label the individual tubes in the  
184 strip with the respective sample identifiers and make sure the marked wells are in the  
185 same 1-8 sequence direction at all times. Use the protocol images to ensure accurate  
186 placement of strip tubes and double check tube placements regularly. RNA extraction,  
187 Poly A selection and Library preparation should be done on the same day.

##### 188 189 **IV.i. Poly A selection protocol**

- 190  
191 1. Verify that the volumes of RNA samples are at least 50 µl using micropipettes  
192 and pipette them into a strip tube (Fisher scientific 14-222-252). Label tube as  
193 “RNA samples”. Spin down in a tabletop mini-centrifuge and keep on ice until  
194 step 7.
- 195 2. Wipe the inner surface of the Apollo system with RNase zap (Thermo Fisher  
196 AM9780) and 70% Ethanol.
- 197 3. Ensure the trash container is empty. The machine shows an error when trash is  
198 full.
- 199 4. Cool the Apollo machine to 4°C using the standard protocol ‘cooling’ function.
- 200 5. Place empty reservoirs (Apollo 640087) in Block-6 row 1 and 2.
- 201 6. Fill Block-5 row 1,2 and 3 with filter tips (Apollo 640084).
- 202 7. Place a new microplate in Block-2.
- 203 8. In two new reservoirs, add 10 ml (protocol says 4/5ml) of Reagent 1 and place it  
204 in row 1 and 10ml of reagent 2 in row 2.
- 205 9. Place empty 8 strip tubes in Block-3 row 4 and 5 and in Block-4 row 1, 2 and 3.
- 206 10. Label an empty strip tube as “products” and place it in Block-3 row 8. This strip  
207 tube will contain the poly-A selected mRNA at the end of this run. Label each  
208 tube with the sample names.
- 209 11. Aliquot 80µl of Reagent 3 (it is a clear solution) into an 8 well strip tube into wells  
210 corresponding to the RNA sample. Label as “Reagent 3” to distinguish it from  
211 RNA samples.
- 212 12. Place Reagent 3 strip tube into Block-3 row 3.
- 213 13. Gently pipette the magnetic bead reagent 4 until it is uniformly resuspended.  
214 Aliquot 15 µl into the same number and locations of the strip tube containing  
215 RNA sample.
- 216 14. Place the RNA sample tube in Block-3 row 1.
- 217 15. At last place the magnetic bead reagent 4 in Block-3 row 2. Place retainers for  
218 Blocks 3 and 4 and lock them.
- 219 16. Restart the machine by switching off and on. On the touchscreen navigate to the  
220 latest version of PolyA8 protocol (“User Maintenance” >  
221 “PrepX\_PolyA8\_betaV2”).
- 222 17. The run lasts for 45 minutes, during which time the reagent mixes for the  
223 subsequent library preparation protocol (**IV.ii**) should be set up.
- 224 18. Remove strip tubes while checking for uniform volumes. Note any discrepancies.

- 225 19. Check the volume of the “product” tube, cap it and spin it in a minispin. The  
226 volume should be approximately 19µl. Cap and store on ice until the next step.  
227 This mRNA “product” strip tube will be used as “sample” in the cDNA library  
228 preparation step.  
229

#### 230 **IV.ii. PrepX mRNA8 Library preparation protocol.**

- 231
- 232 1. Prepare the RNase III mix and Reverse Transcription (RT) reaction mix for the  
233 number of mRNA samples and an additional sample.
  - 234 2. In a RNase free tube mix 2µl each of RNase Buffer III and RNase III enzyme  
235 (Thermo Fisher 18080093) per sample required. Pipette gently and give a brief  
236 spin on a tabletop mini-centrifuge. Leave the tube on ice.
  - 237 3. Mix the following reagents per reaction to make the RT reaction mix and place it  
238 on ice:
    - 239 • 5X First strand buffer 16µl
    - 240 • 0.1M DTT 08µl
    - 241 • dNTP 04µl
    - 242 • Superscript III Reverse Transcriptase 02µl
    - 243 • Murine RNase inhibitors 01µl

244

245 Setting the apollo system blocks:

- 246
- 247 4. Place empty strip tubes in Block-3 rows 1 and 2 and in Block-4 row 6.
  - 248 5. Label a strip tube as products and place it in Block-3 row 5.
  - 249 6. Fill filter tips in Block-5 rows 1-7, fill black piercing tips (Apollo 640085) in row 12.
  - 250 7. Fill 1.1 ml tube strips in Block-1 row 1,2 and 3.
  - 251 8. Place a used microplate in Block-2.
  - 252 9. Cool the Apollo machine to 4°C using standard protocol ‘cooling’ function.
  - 253 10. Place empty reservoirs in position 2 and 4 of Block-6. Add 15 ml of 100%  
254 molecular grade ethanol (Sigma E7023) in reservoir 3 and 15 ml of nuclease free  
255 water (part of Takara library prep kit 640096) in reservoir 1.
  - 256 11. In a new strip tube, aliquot 4 µl of RNase III mix into each tube corresponding to  
257 the sample and place it in Block-4 row 5.
  - 258 12. In a new strip tube, aliquot 31 µl of RT reaction mix into each corresponding  
259 sample tube and place it in Block-4 row 7.
  - 260 13. Gently pipette A-line beads and aliquot 200µl into a fresh strip tube at the  
261 corresponding wells to that of the sample and place it in Block-4 row 8.
  - 262 14. Thaw blue enzyme and orange adapter/primer strips of the PrepX mRNA8 kit  
263 (Takara 640096) on ice. The number of these strips is the same as the sample  
264 number. Flick the bottom of tubes to dislodge liquid and mix uniformly. Spin down  
265 and place it back on ice.
  - 266 15. Sometimes a solid precipitate might be visible in the enzyme strip tubes. It  
267 generally dissolves after flicking. Do not use the strip if it is not soluble after  
268 thawing and mixing.
  - 269 16. Place the Blue strip tubes with the arrow pointing up in Block4 rows 9-12 in  
270 columns corresponding to the mRNA samples.

- 271 17. Place the orange strip tubes in Block-4 from row 1-4 in columns corresponding to  
 272 the mRNA sample tubes.
- 273 18. Verify the filter and piercing tips in Block-5, 1.1ml tubes in Block-1, mock  
 274 microplate in Block-2, Reservoir 3 with 100% ethanol and Reservoir-1 with  
 275 Nuclease free water, Reservoirs 4-5 empty place holders, three sets of empty  
 276 tubes (one for cDNA products) and mRNA sample tube in Block-3 and in Block-4  
 277 Blue and orange strips, one empty strip tube, RT, RNase III and bead strip tubes  
 278 in specified locations.
- 279 19. Lock Block-3 and 4 with retainer plates.
- 280 20. In the touchscreen control select User maintenance > Run the protocol  
 281 'PrepX\_mRNA8\_200bp\_BetaV1.scb. The screen does not show any progress  
 282 bar. This program runs for 5 hours.
- 283 21. cDNA after this step is fairly stable and can be processed the next day. Keep at  
 284 4°C until processing.

285  
 286 **IV.iii. PCR Amplification of the Libraries.**

- 287
- 288 1. Check the volume of the “product” tube, cap it and spin it in a minispin. The  
 289 volume should be around 19µl. Cap and store on ice until the next step.
  - 290 2. Prepare PCR master mix with 25µl long Amp Taq (NEB M0323S) and 2.5 µl of  
 291 SR primer per sample on ice.
  - 292 3. Add unique index primers (PrepX RNAseq index 1-48) to each of the cDNA  
 293 products and add the PCR master mix. Make up the total volume in each tube to  
 294 50µl with Nuclease free water.
  - 295 4. Mix well and spin down. Place the strip tube in a PCR machine and run a 15  
 296 cycle PCR amplification reaction as shown below:

<b>Temp</b>	94°C	94°C	60°C	65°C	65°C	10°C
<b>Time</b>	60 sec	30 sec	30 sec	30 sec	7 min	hold
<b>Cycles</b>		----- 14 x -----			extension	

- 298
- 299 6. After completion of PCR cool the samples and spin down.
  - 300 7. PCR Cleanup using the Apollo system PrepX\_PCR clean up8 protocol.
  - 301 8. Cool the Apollo machine to 4°C using standard protocol ‘cooling’ function.
  - 302 9. Place filter tips in Block-5 row 1. Block-6 is similar to the library preparation  
 303 protocol, empty reservoirs in position 2 and 4 of Block-6. 10 ml of 100% molecular  
 304 grade ethanol (Sigma E7023) in reservoir 3 and 15 ml of nuclease free water (part  
 305 of Takara library prep kit 640096)) in reservoir 1.
  - 306 10. Place empty strip tubes in Block-3 row 2 and 3. Label a strip tube as “cleaned  
 307 cDNA product” and place it in row 4. Place the amplified cDNA samples in row 1.
  - 308 11. Aliquot 50 µl of A-line beads into a fresh strip tube at corresponding locations to the  
 309 samples. Place this tube in the end of the set up.
  - 310 12. Place retainers on Block-3 and 4 and lock it.

- 311 13. Run Utility apps> PCR cleanup 8 protocol on touch screen. The run lasts 20  
312 minutes.
- 313 14. Check volumes of the cleaned 'product' tube. Spin down and place on ice.
- 314 15. Run Qubit to quantify the cDNA with the high sensitivity DNA kit. Use a TapeStation  
315 to run the gel and measure cDNA quantity using ladder and high sensitivity tape  
316 (Agilent 5067-5579). Depending on the qubit quantification, higher concentrations  
317 use DNA 1000 tape (Agilent 5067-5582).
- 318 16. Transfer the cDNA in strip tubes to a lobind RNA tube (Eppendorf 8077-230) and  
319 label them with details about the sample-genotype, date of cDNA prep, it is a  
320 cDNA library, the concentration of the sample, and the volume of sample  
321 remaining after quantification. Store at -80°C until it is ready to be sequenced.
- 322 17. Calculate the total molar concentration of the lane and the dilution needed for  
323 each library to make it equimolar. Mix the volumes in a single lobind tube and  
324 submit to the sequencing facility.  
325

326  
327

**KEY RESOURCES TABLE**

REAGENT or RESOURCE	SOURCE	IDENTIFIER
<b>Chemicals</b>		
Hoechst 33342	Thermo Fisher	Cat# H1399
Dulbecco's Phosphate Buffered Saline PBS	Thermo Fisher	Cat# 14190144
Trypsin 0.25%	Thermo Fisher	Cat# 25200056
Liberase 2.5%	Sigma	Cat# 5401119001
Trizol	Thermo Fisher	Cat# 15596206
Ethanol molecular 200 grade	Sigma	Cat# E7023
Nuclease free water	Thermo Fisher	Cat# 10977015
Magnetic Beads	A-line	Cat# C1003
Triton X100	VWR	Cat# 97062-208
<b>Critical Commercial Assays</b>		

Zymo RNA Micro-prep kit	Zymo Research	Cat# R2060
Superscript III Reverse Transcriptase	Thermo Fisher	Cat# 18080093
Takara PrepX PolyA-8	Takara	Cat# 640098
Takara PrepX mRNA-8	Takara	Cat# 640096
Qubit RNA HS Assay Kit	Thermo Fisher	Cat# Q32852
Qubit DNA HS Assay Kit	Thermo Fisher	Cat# Q32854
LongAmp Taq DNA Polymerase	New England BioLabs	Cat# M0287S
<b>Deposited Data</b>		
Raw and analyzed data	This paper	GEO: GSE172015
<b>Experimental Models: Organisms/Strains</b>		
<i>D. melanogaster</i> . bab1 GAL4: w[*]; P{w[+mW.hs]=GawB}bab1[PGAL4-2]/TM6B, Tb[1]	Bloomington Drosophila Stock Center	BDSC:6803; FlyBase:ID FBst0006803
<i>D. melanogaster</i> . nos GAL4: P{w[+mC]=UAS-Dcr-2.D}1, w[1118]; P{w[+mC]=GAL4-nos.NGT}40	Bloomington Drosophila Stock Center	BDSC:25751; FlyBase: ID FBst0025751

<i>D. melanogaster. w1118, P{UAS Stinger}</i>	(BAROLO <i>et al.</i> 2000)	UAS Green Stinger on X
<b>Instruments</b>		
MoFlo Astrios EQ Cell sorter	Beckman Coulter	B25982
Motorized pellet pestle	Kimble	Cat# 749540-0000
NanoDrop	Nanodrop	ND1000
Qubit 3.0 Fluorometer	Thermo Fisher	Cat# Q33216
Tapestation	Agilent	2200/4200
PCR Thermal cycler	Bio-Rad	C1000
Illumina Hi Seq	Illumina	2500
<b>Consumables</b>		
Insulin Syringe	Becton Dickinson	Cat# 328418
RNA lo-bind tubes	Eppendorf	Cat# 8077-230
High Sensitivity RNA ScreenTape	Agilent	Cat# 5067-5579

High Sensitivity DNA ScreenTape	Agilent	Cat# 5067-5584
DNA 1000 ScreenTape	Agilent	Cat# 5067-5582
Axygen PCR 8-strip tubes	Fisher Scientific	Cat# 14-222-252
Apollo Filter tips 300027	Takara	Cat# 640084
Apollo Piercing tips 300028	Takara	Cat# 640085
Apollo Reservoirs 300031	Takara	Cat# 640087
<b>Software and Algorithms</b>		
Drosophila melanogaster genome version	(LARKIN <i>et al.</i> 2021)	Dmel_r6.36_FB2020_05
RSEM v 1.3.3	(LI AND DEWEY 2011)	<a href="https://deweylab.github.io/RSEM/">https://deweylab.github.io/RSEM/</a>
STAR aligner v 2.7.6a	(DOBIN <i>et al.</i> 2013)	<a href="https://github.com/alexdobin/STAR">https://github.com/alexdobin/STAR</a>
DESeq2 v 1.26.0	(LOVE <i>et al.</i> 2014)	<a href="https://bioconductor.org/packages/release/bioc/html/DESeq2.html">https://bioconductor.org/packages/release/bioc/html/DESeq2.html</a>
Bcl2fastq2 v2.20		<a href="https://support.illumina.com/downloads/bcl2fastq-conversion-software-v2-20.html">https://support.illumina.com/downloads/bcl2fastq-conversion-software-v2-20.html</a>

329 **SUPPLEMENTARY REFERENCES**

330

331 Barolo, S., L. A. Carver and J. W. Posakony, 2000 GFP and beta-galactosidase  
332 transformation vectors for promoter/enhancer analysis in *Drosophila*.  
333 *Biotechniques* 29: 726, 728, 730, 732.

334 Dobin, A., C. A. Davis, F. Schlesinger, J. Drenkow, C. Zaleski *et al.*, 2013 STAR: ultrafast  
335 universal RNA-seq aligner. *Bioinformatics* 29: 15-21.

336 Larkin, A., S. J. Marygold, G. Antonazzo, H. Attrill, G. Dos Santos *et al.*, 2021 FlyBase:  
337 updates to the *Drosophila melanogaster* knowledge base. *Nucleic Acids Res* 49:  
338 D899-D907.

339 Li, B., and C. N. Dewey, 2011 RSEM: accurate transcript quantification from RNA-Seq  
340 data with or without a reference genome. *BMC Bioinformatics* 12: 323.

341 Love, M. I., W. Huber and S. Anders, 2014 Moderated estimation of fold change and  
342 dispersion for RNA-seq data with DESeq2. *Genome Biol* 15: 550.

343 Slaidina, M., T. U. Banisch, S. Gupta and R. Lehmann, 2020 A single-cell atlas of the  
344 developing *Drosophila* ovary identifies follicle stem cell progenitors. *Genes Dev*  
345 34: 239-249.

346

347

348

349 **SUPPLEMENTARY TABLE LEGENDS**

350

351 **Supplementary Table S1:** RNA-seq sample metadata, including the sample name,  
352 biological and technical replicate information, tissue, stage, cDNA concentration, PrepX  
353 Index used, number of ovaries used, number of cells counted by FACS (not applicable to  
354 whole ovary samples), number of raw reads, aligned reads, and percentage of aligned  
355 reads as reported by the RSEM summary.

356

357 **Supplementary Table S2:** Differentially expressed genes ( $p_{adj} < 0.01$ ) between the  
358 consecutive developmental stages of whole ovary libraries. The column “Contrast”  
359 indicates whether the gene was found differentially expressed in early vs mid stages or  
360 mid vs late stages, and the column “Up\_in” indicates which library the gene was  
361 overexpressed in.

362

363 **Supplementary Table S3:** Differentially expressed genes ( $p_{adj} < 0.01$ ) at each stage  
364 compared to the other two stages of the whole ovary. The column “Stage\_up” indicates  
365 which stage the given gene was overexpressed in.

366

367 **Supplementary Table S4:** Differentially expressed genes ( $p_{adj} < 0.01$ ) between germ  
368 cells and somatic cells at all studied stages. The column “Up\_in” indicates whether the  
369 gene was found upregulated in germ cells or somatic cells.

370

371 **Supplementary Table S5:** Differentially expressed genes ( $p_{adj} < 0.01$ ) between germ  
372 cells and somatic cells at each individual stage. The column “Up\_in” indicates whether  
373 the gene was found upregulated in germ cells or somatic cells, and the column “Stage”  
374 indicates the stage (early, mid or late) in which the test was performed.

375

376 **Supplementary Table S6:** Differentially expressed genes ( $p_{adj} < 0.01$ ) between the  
377 consecutive developmental stages of somatic cell libraries. The column “Transition”  
378 indicates whether the gene was found differentially expressed in the transition from early  
379 to mid-stage or from mid to late stage, and the column “Up\_Down” indicates whether the  
380 gene was up or down regulated in the given transition.

381

382 **Supplementary Table S7:** Differentially expressed genes ( $p_{adj} < 0.01$ ) at each stage  
383 compared to the other two stages of the somatic tissue library. The column “Stage\_up”  
384 indicates the stage that a given gene was found overexpressed at.

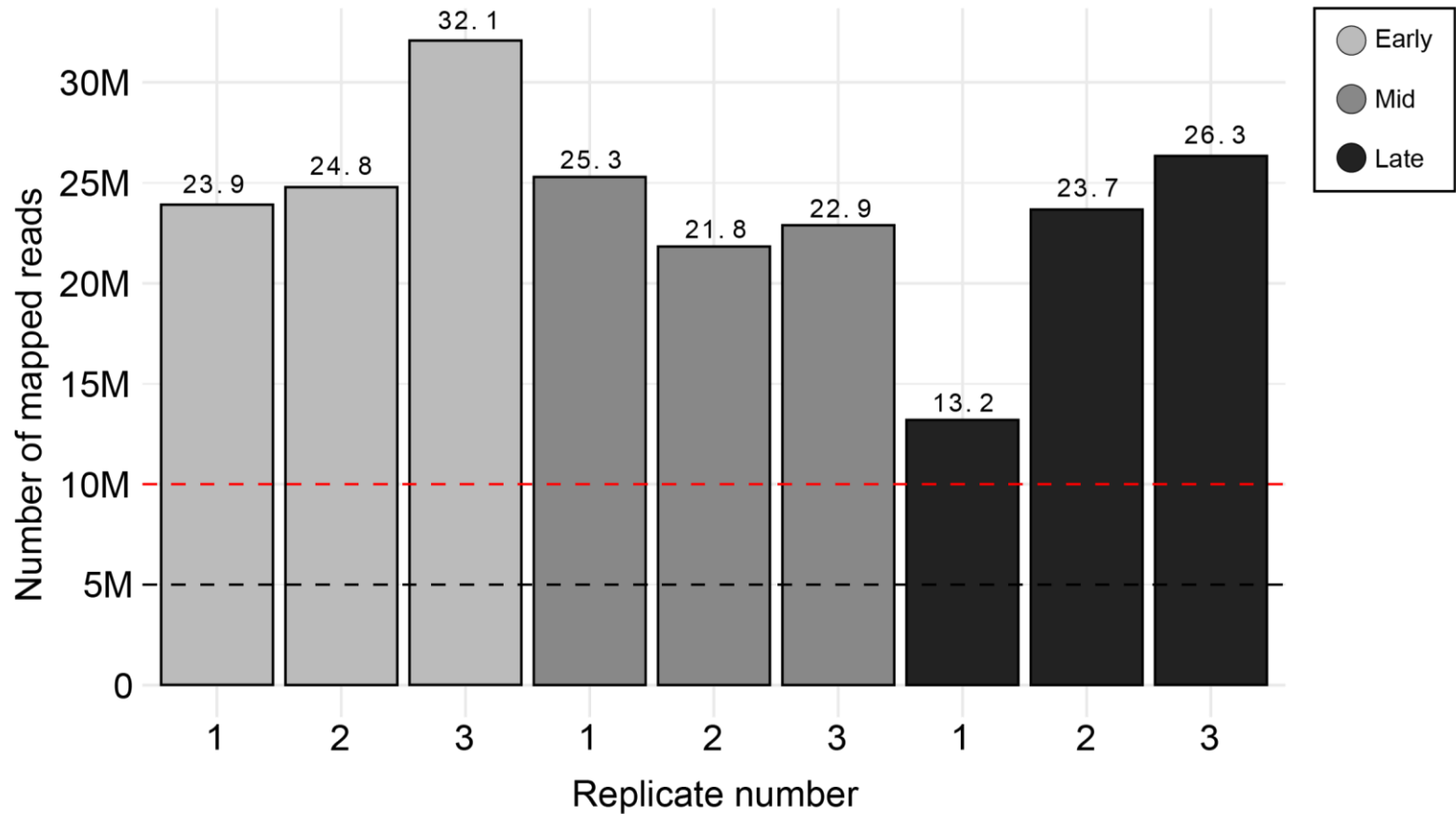
385

386 **Supplementary Table S8:** Differentially expressed genes ( $p_{adj} < 0.01$ ) between the  
387 consecutive stages of germ cell libraries. The column “Transition” indicates whether the  
388 gene was found differentially expressed in the transition from early to mid-stage or from  
389 mid to late stage, and the column “Up\_Down” indicates whether the gene is up or down  
390 regulated in the given transition.

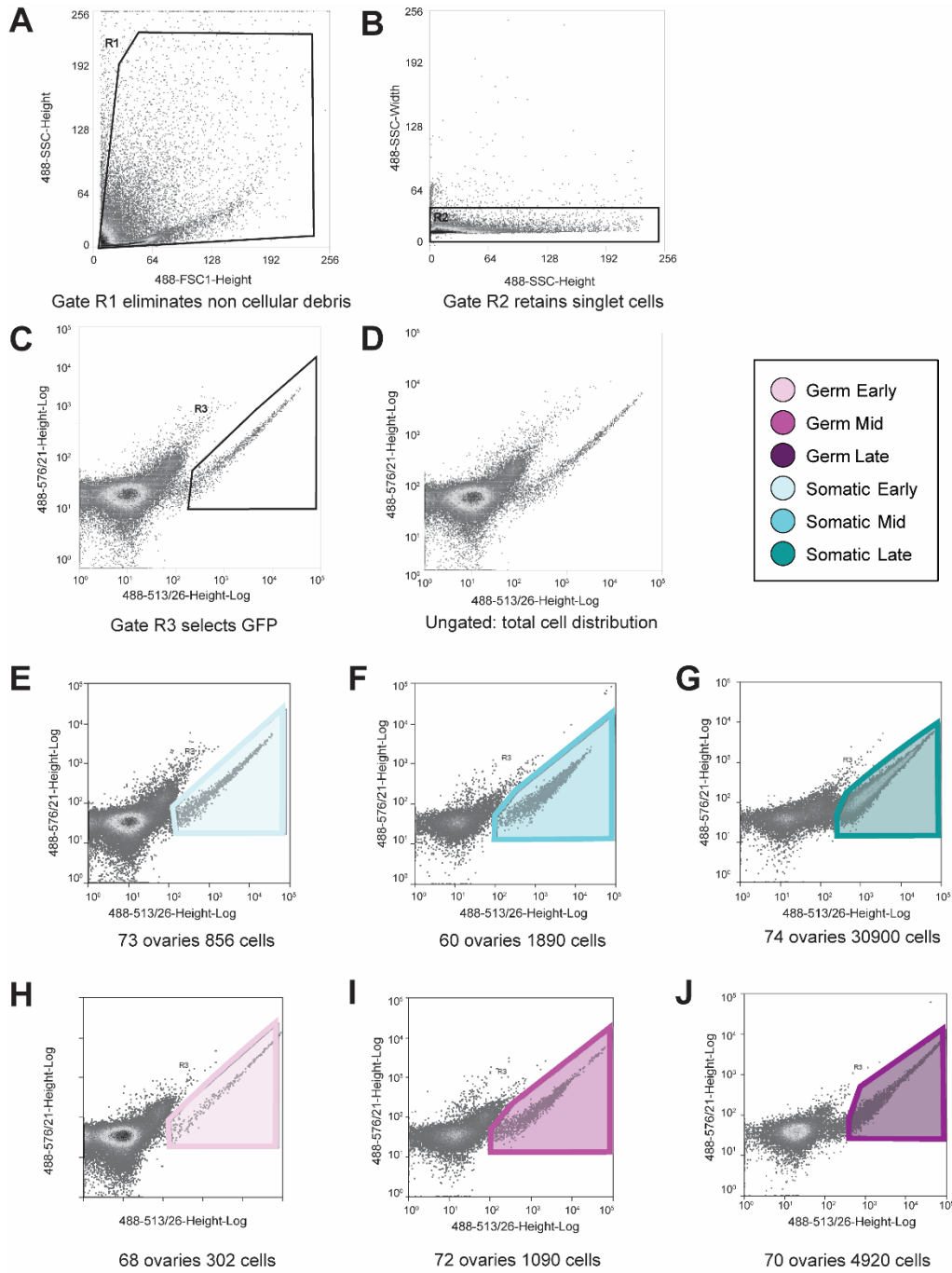
391

392 **Supplementary Table S9:** Differentially expressed genes ( $p_{adj} < 0.01$ ) at each stage  
393 compared to the other two stages of the germ cell library. The column “Stage\_up”  
394 indicates the stage at which the given gene was found to be overexpressed.

395 SUPPLEMENTARY FIGURES AND LEGENDS  
396



397  
398 **Supplementary Figure S1.** Number of aligned reads in each of three biological replicates of whole ovary RNA-seq samples.  
400 The Black dashed line: five million reads; red dashed line: ten million reads.  
401



403

404

405 **Supplementary Figure S2.** Representative FACS cell density plots of GFP-positive cell

406 sort from dissociated ovaries showing gating scheme used to obtain GFP-positive singlet

407 cell population. A) Elimination of cellular debris using R1 (cells out of R1) gate. B)

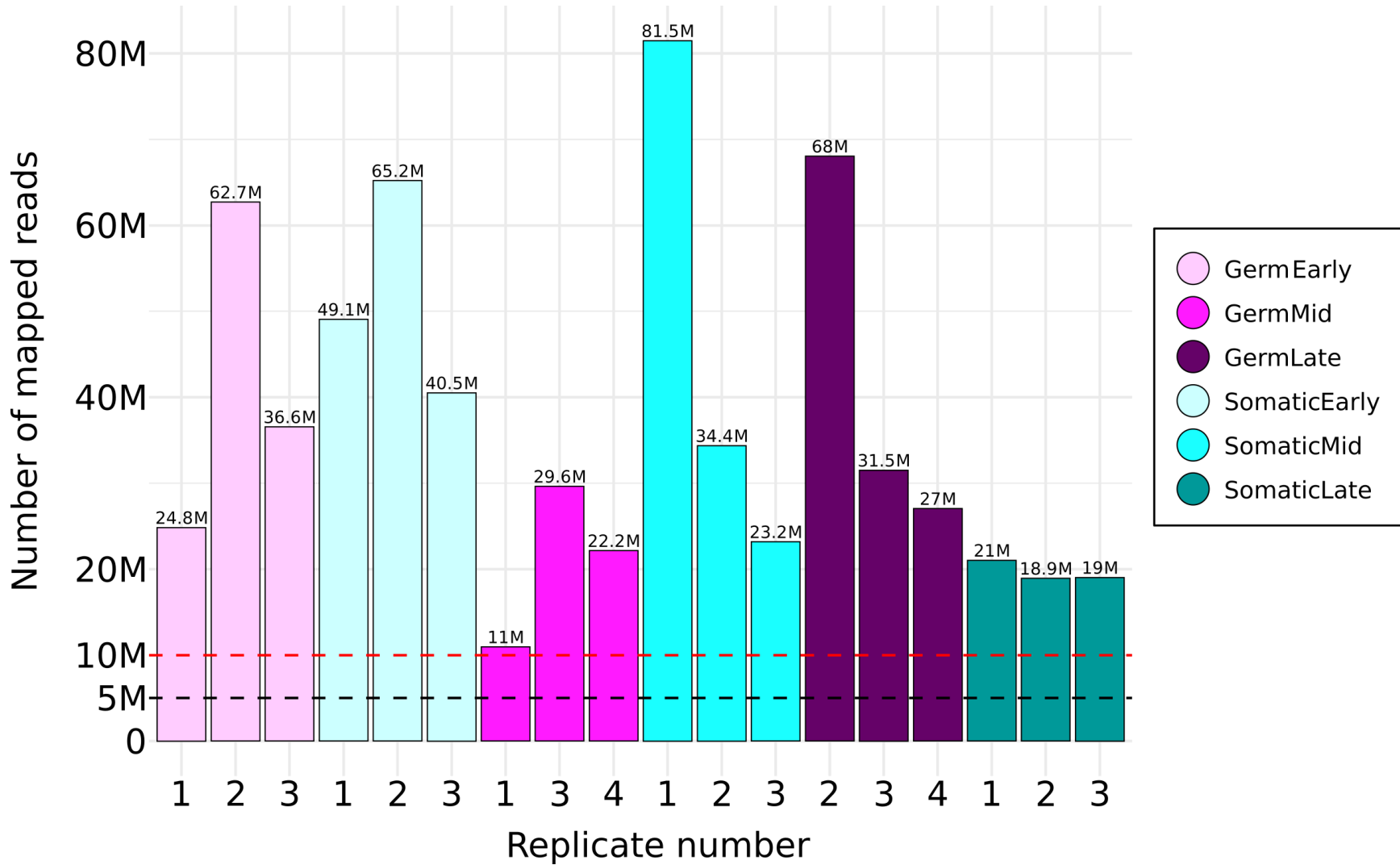
408 Elimination of non-singlets (cells outside R2) using R2 gate. C) Selection of GFP-positive

409 cells through R3 (cells inside R3) gate. D) Ungated plot showing distribution of all cells.

410 E-J) Representative R3 gated plots showing number of GFP-positive cells for similar

411 number of ovaries.

412

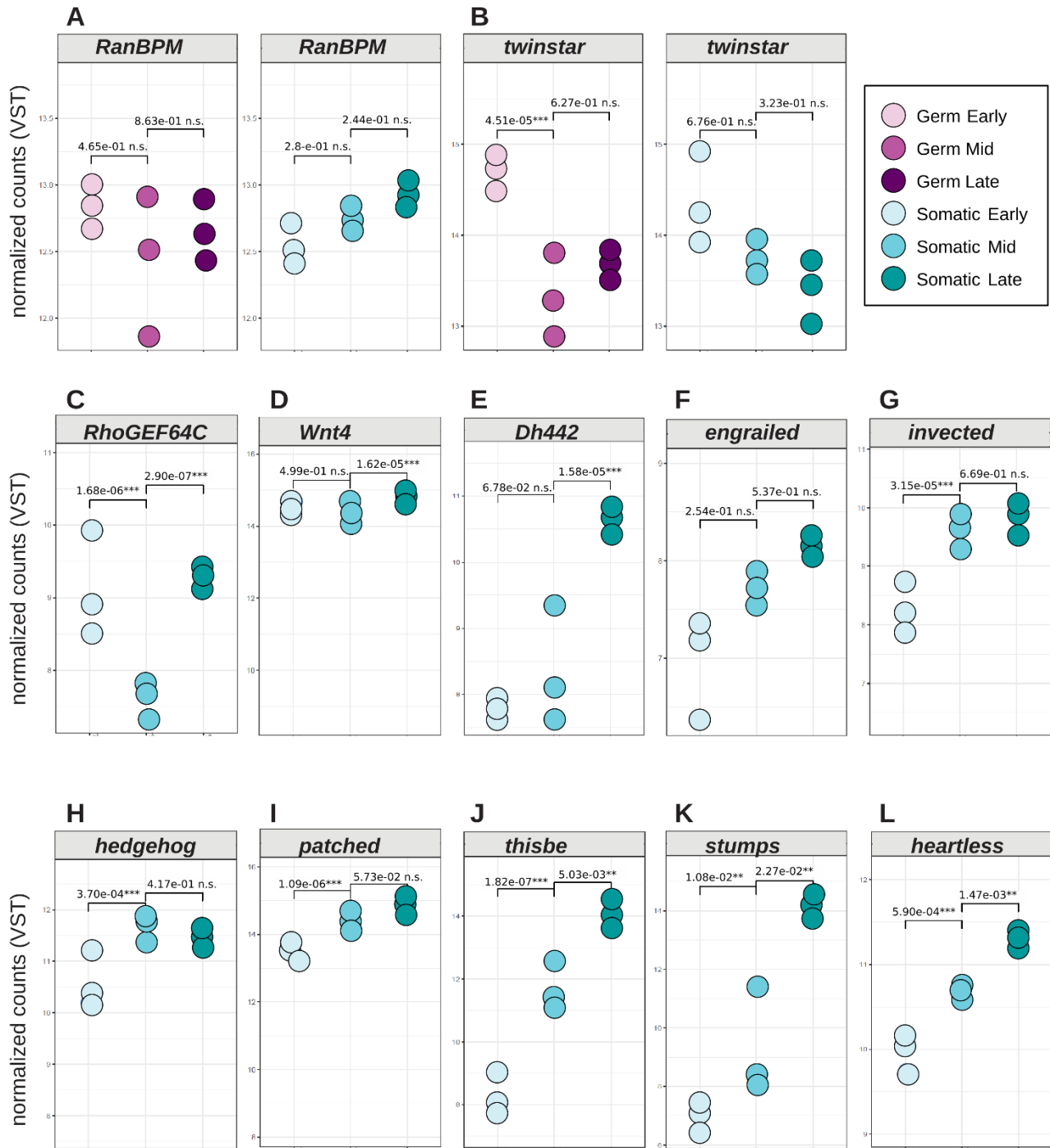


413

414

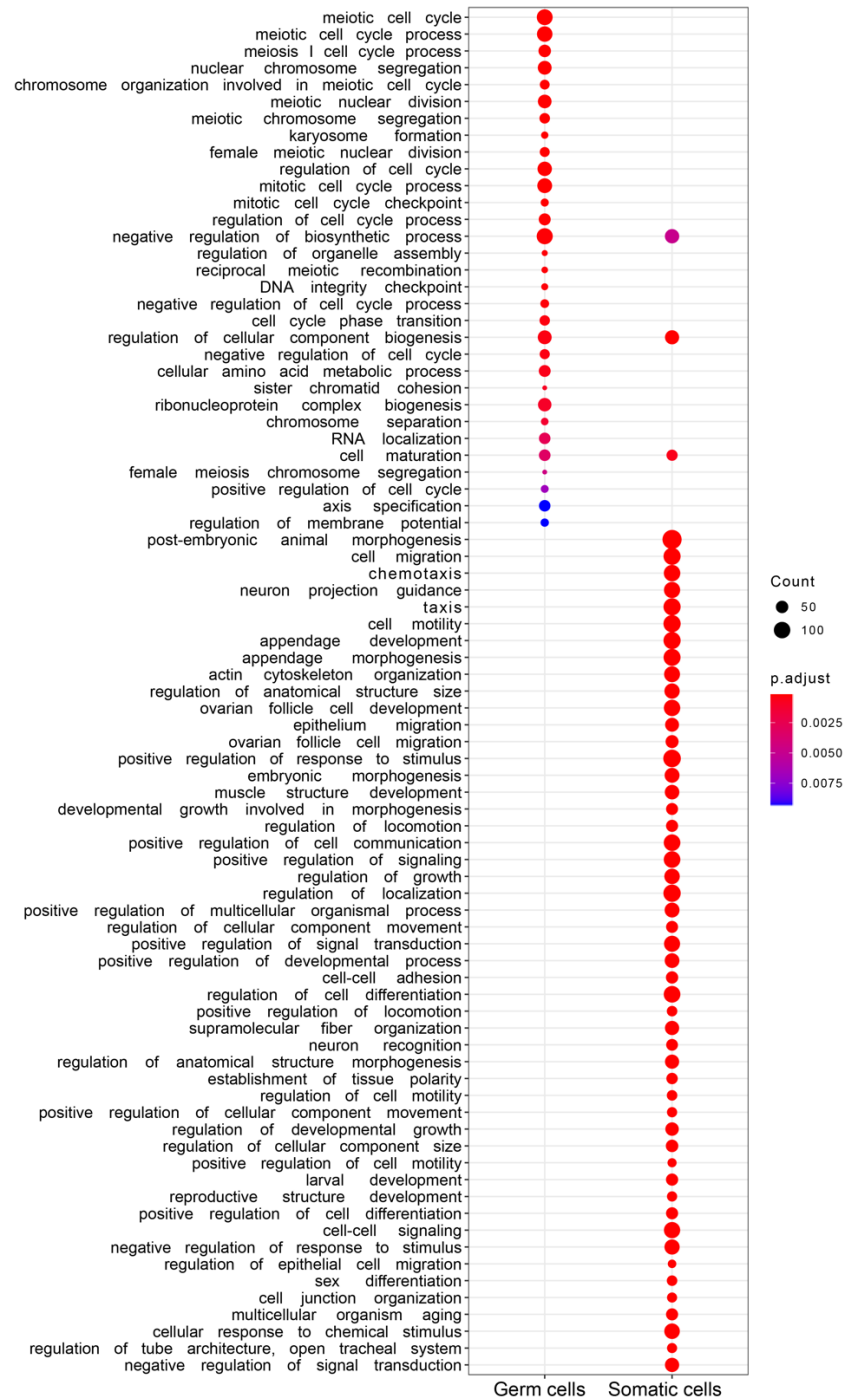
415

**Supplementary Figure S3.** Number of aligned reads in each of three tissue-specific biological replicate samples used for the analyses presented in this study. Black dashed line: five million reads; red dashed line: ten million reads.



417  
418  
419  
420  
421

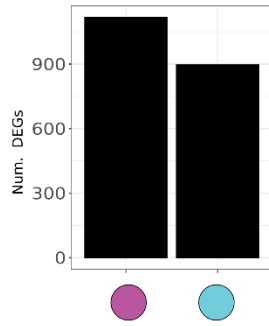
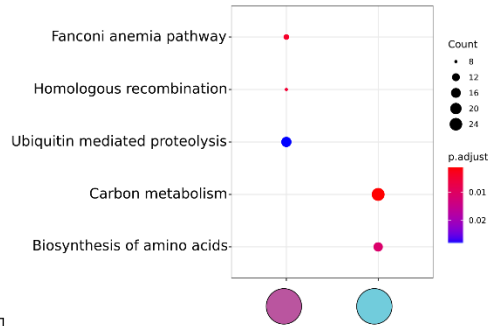
**Supplementary Figure S4.** Dot plots of genes differentially expressed across stages. Expression in VST counts of genes in each tissue-specific RNA-seq library. The adjusted p-values shown were calculated in the differential expression analysis with DESeq2. \*p-value<0.05, \*\*p-value<0.01, \*\*\*p-value<0.001, n.s. not significant



423  
424  
425  
426  
427  
428  
429

**Supplementary Figure S5.** Gene Ontology terms (GO-terms) for Biological Process level 4 that were significantly enriched (BH adjusted p-value<0.01, minimum number genes with the term=30) within the set of genes differentially expressed (BH adjusted p-value<0.01) between germ cells and somatic cells. The circle size is proportional to the number of genes with the GO-term in the corresponding gene set. The color of the circle indicates the adjusted p-value.



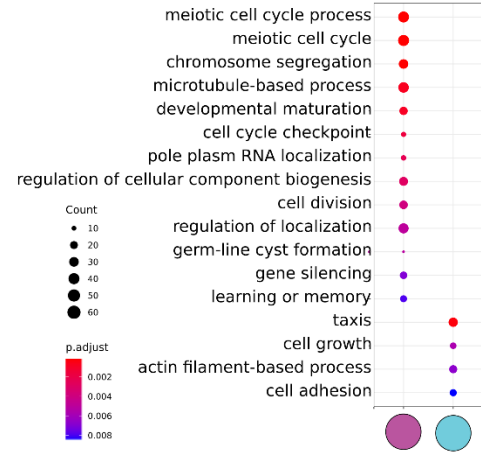
**B****DEA****KEGG**

Count

- 8
- 12
- 16
- 20
- 24

p.adjust

0.01  
0.02

**GO**

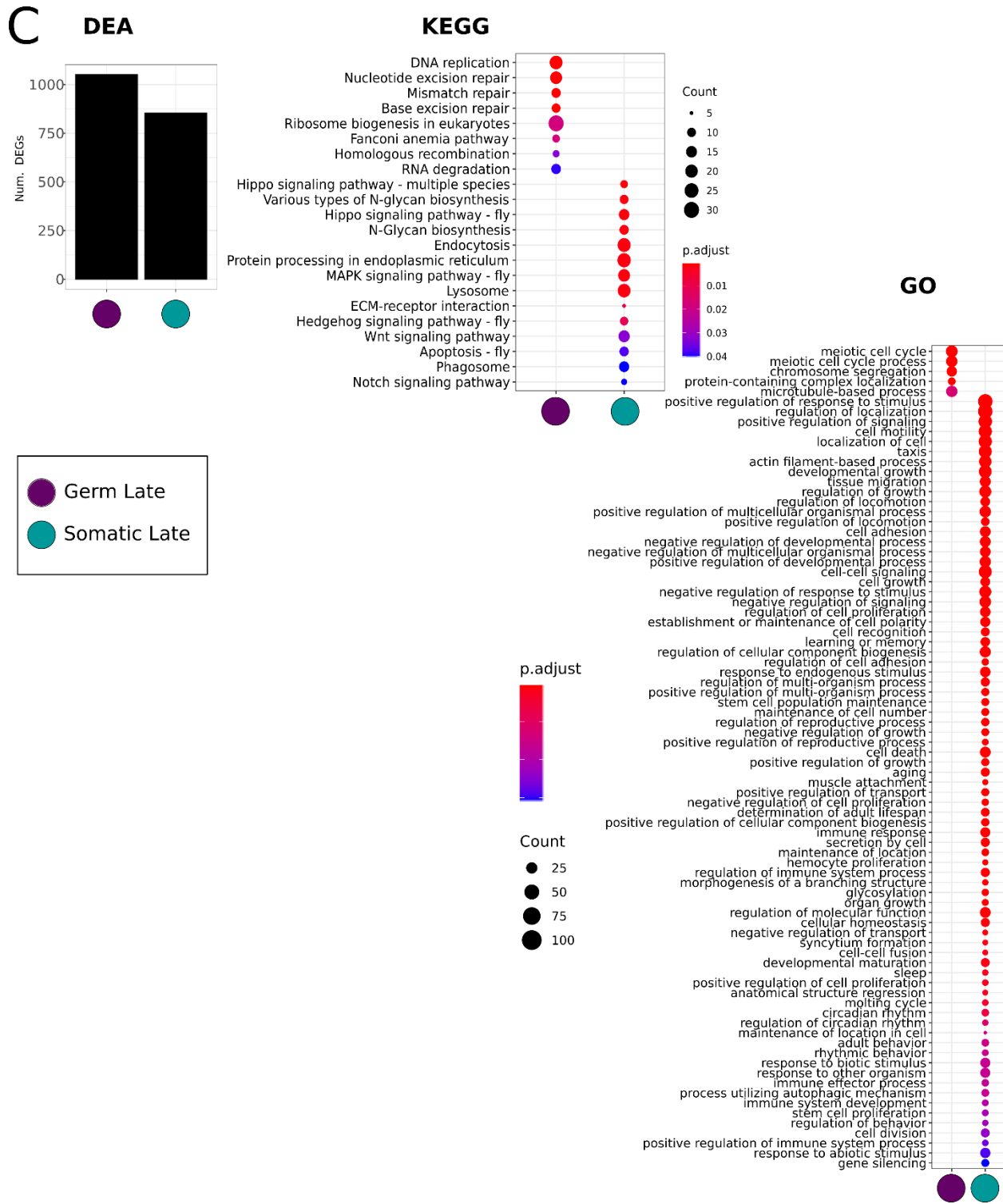
Count

- 10
- 20
- 30
- 40
- 50
- 60

p.adjust

0.002  
0.004  
0.006  
0.008

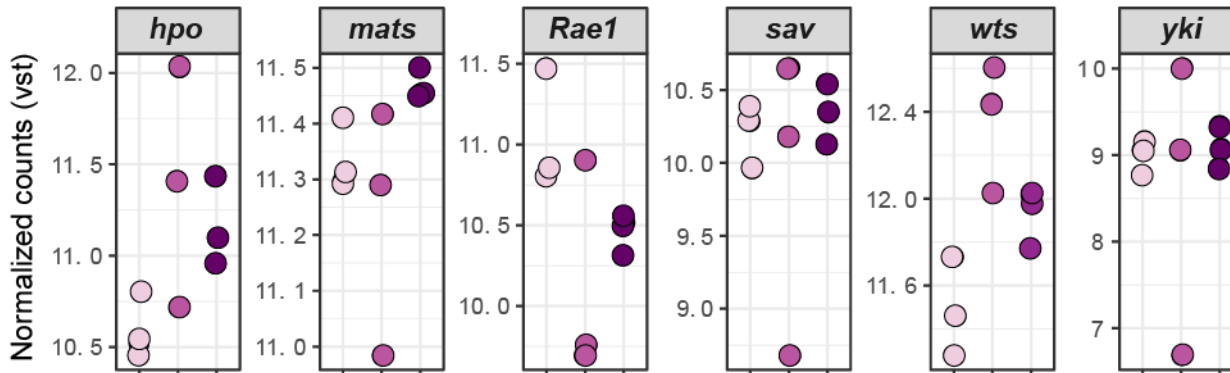
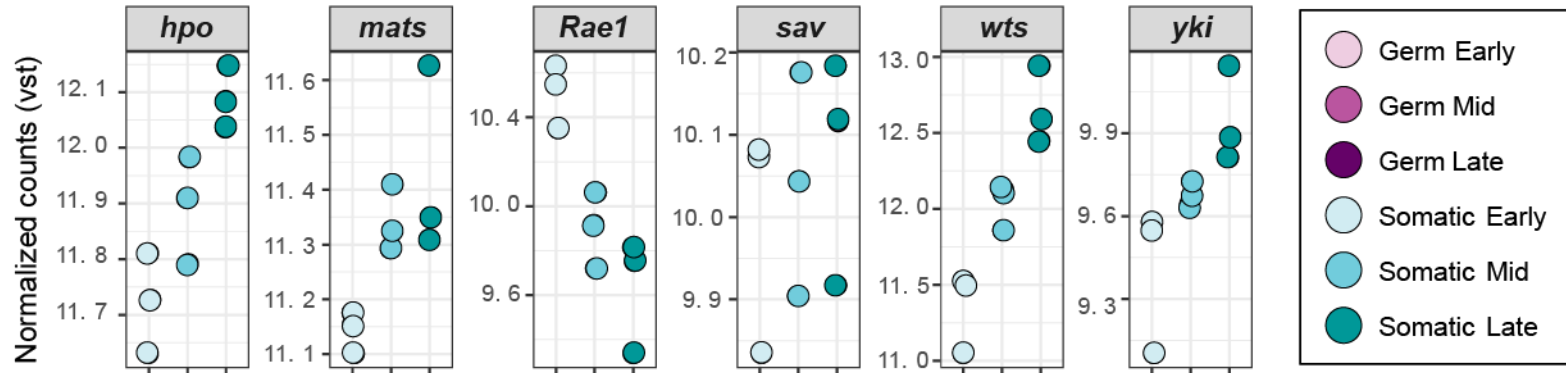
432



433  
434  
435  
436  
437  
438  
439

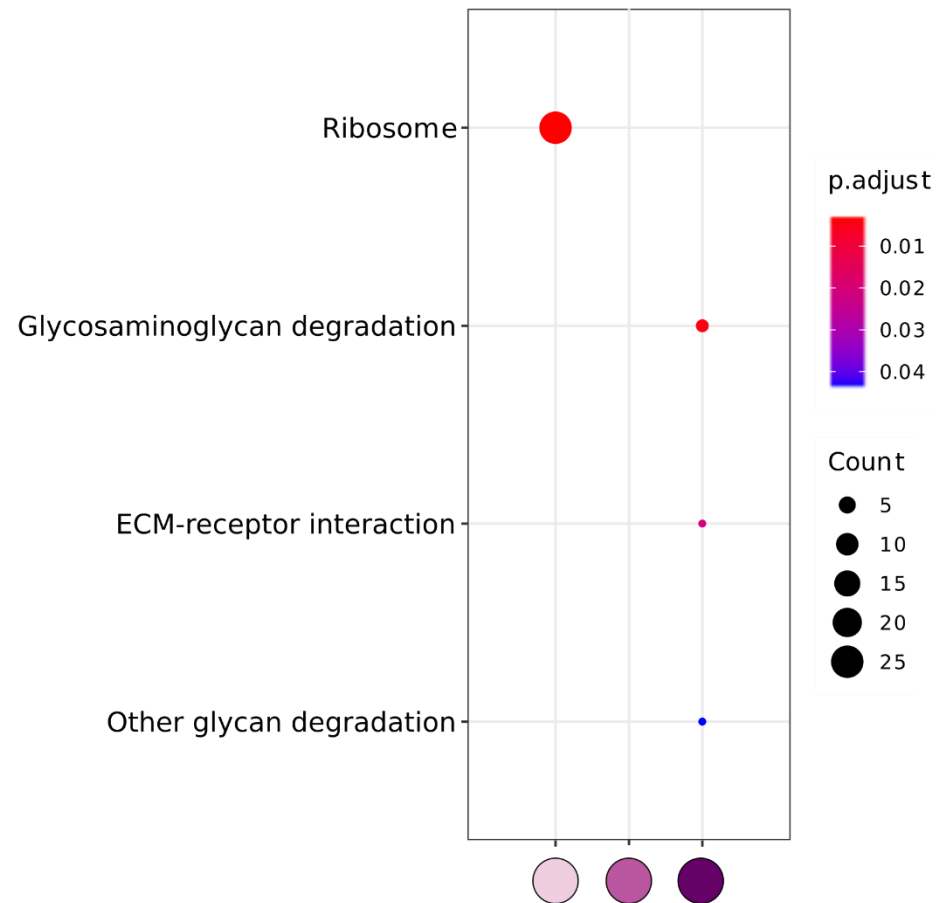
**Supplementary Figure S6.** Number of significantly upregulated genes in germ cells and somatic cells at A) early, B) mid, and C) late stages, and the KEGG pathways and GO-term identified as significantly enriched (BH adjusted p-value<0.05 for KEGG and BH p-value<0.01 for GO) within each set of upregulated genes. See Supplementary Table S5 for gene list.

440



441  
442  
443  
444  
445  
446

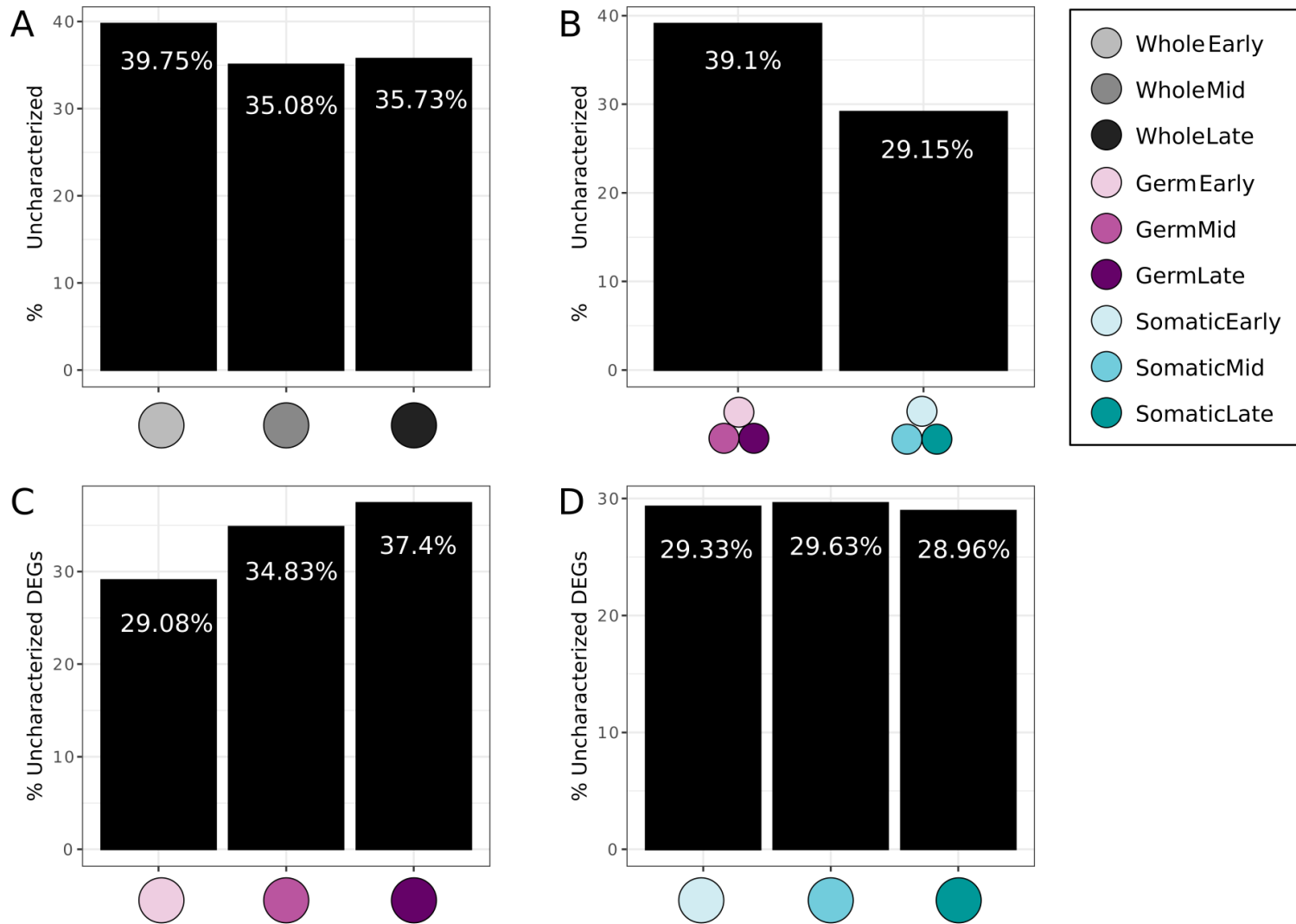
**Supplementary Figure S7.** Expression in VST counts of the Hippo signaling pathway core component genes according to FlyBase (FBgg0000913) in each tissue-specific RNA-seq library. Note that y axes differ slightly between plots



447  
448  
449  
450  
451  
452  
453

**Supplementary Figure S8.** Significantly enriched (BH adjusted p-value<0.05) KEGG pathways within the sets of genes significantly overexpressed (p-value<0.01) in each stage of the germ cell libraries. The circle size is proportional to the number of genes with the GO-term in the corresponding gene set. The color of the circle indicates the adjusted p-value.

454

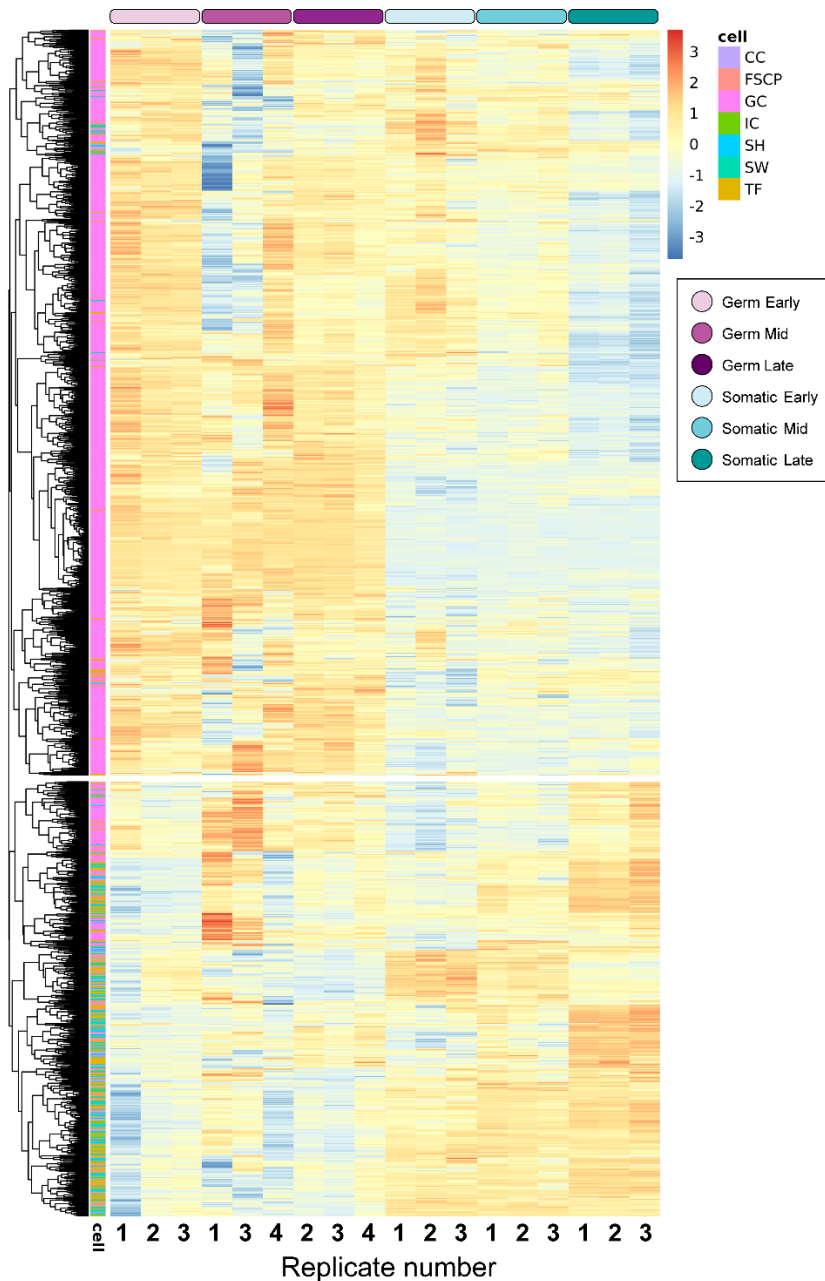


455

456

457

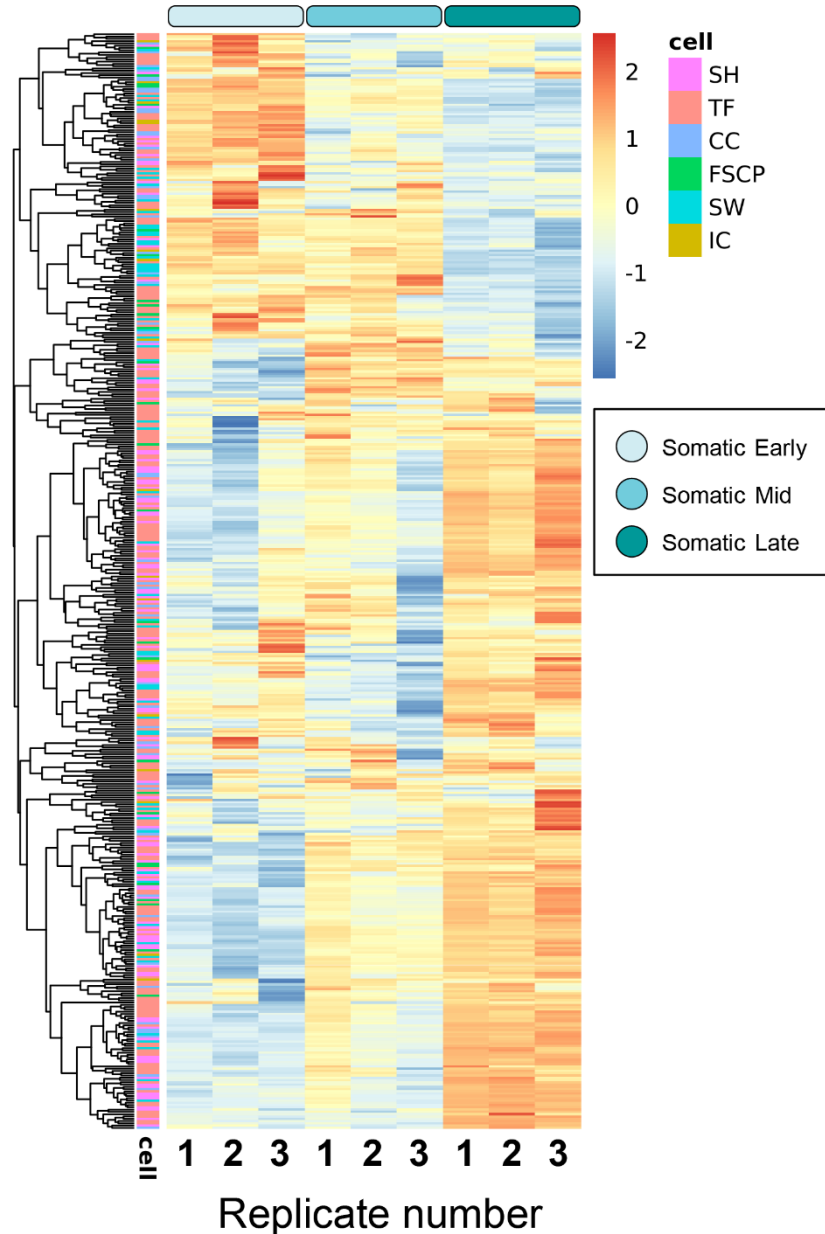
**Supplementary Figure S9.** Uncharacterized genes in differential expression comparisons.



459

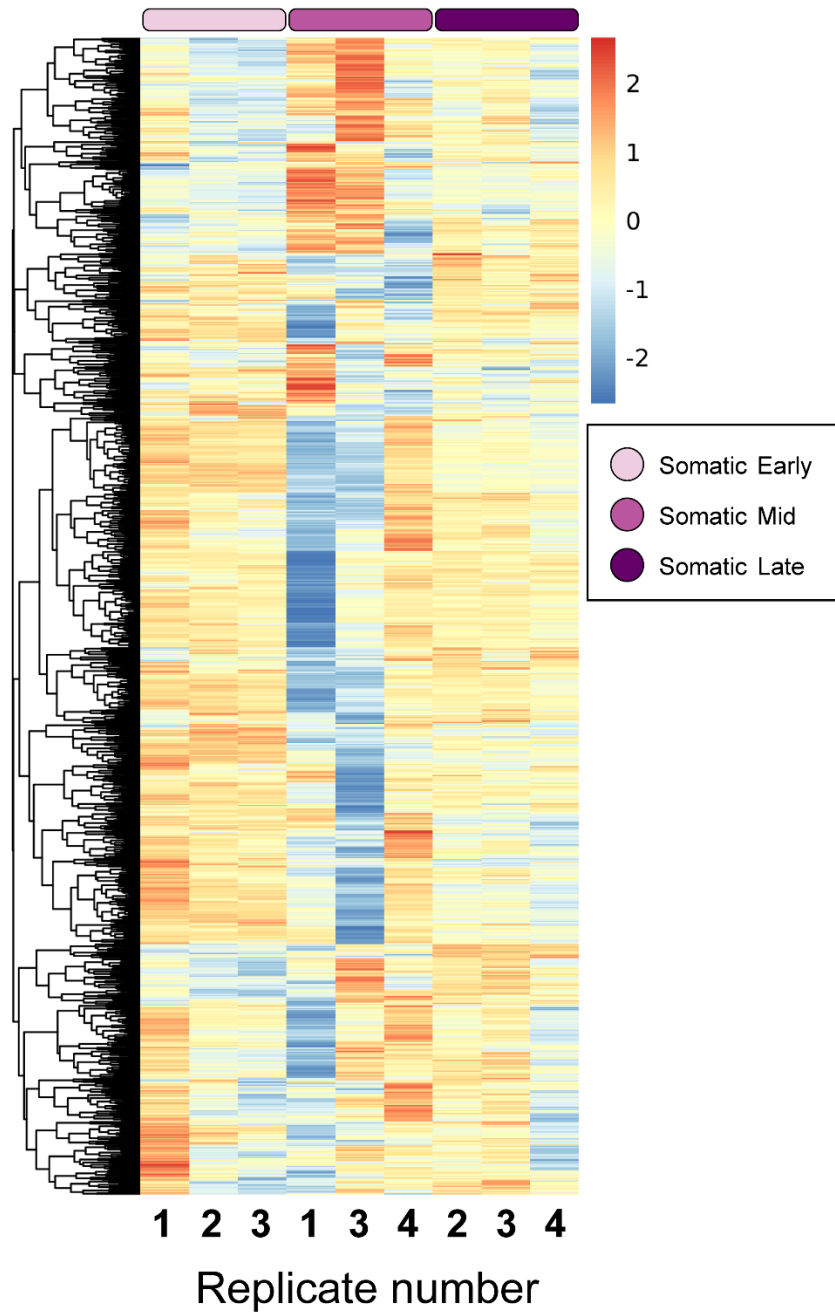
460

461 **Supplementary Figure S10.** Expression across our dataset of the cell markers exclusive  
 462 of a single cell type obtained from SLAIDINA *et al.* (2020). The color of the first indicates  
 463 the cell type of which each gene is a marker of (CC: cap cells, FSCP: follicle stem cells,  
 464 GC: germ cells, IC: intermingled cells, SH: sheath cells, SW: swarm cells, TF: terminal  
 465 filament). Genes are clustered based on hierarchical clustering and separated into two  
 466 groups using the cuttree function which resulted in the separation of the germ cell markers  
 467 from somatic markers. The expression of each gene across samples is represented as a  
 468 row-wise Z-Score value of the VST-normalized counts from high (red) to low (blue).



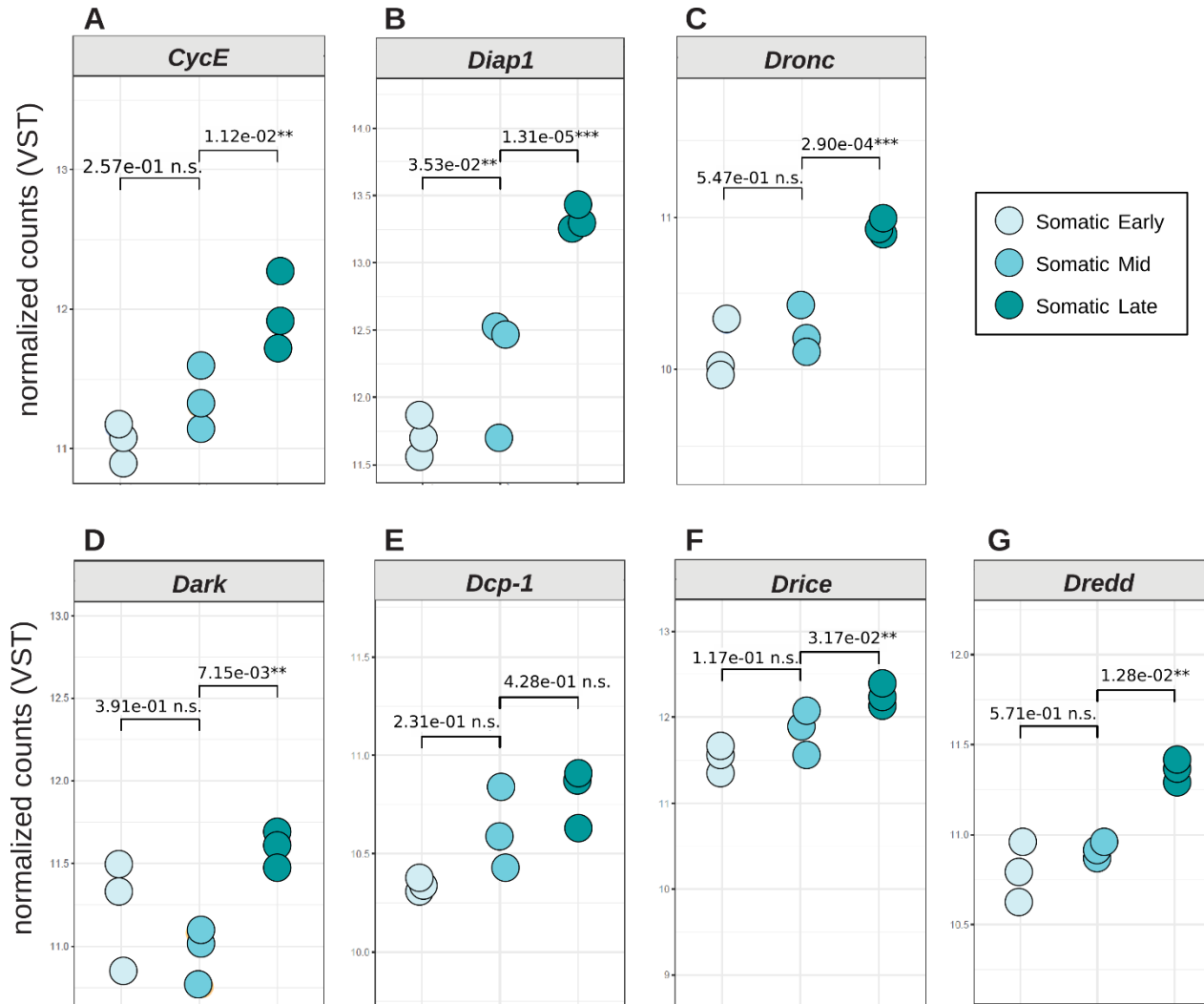
470  
471

472 **Supplementary Figure S11.** Expression across stages in somatic cell libraries of the  
473 somatic markers exclusive of a single cell type obtained from SLAIDINA *et al.* (2020). The  
474 color of the leftmost column indicates the cell type suggested by each marker gene (CC:  
475 cap cells; FSCP: follicle stem cells; GC: germ cells; IC: intermingled cells; SH: sheath  
476 cells; SW: swarm cells; TF: terminal filament). Genes are grouped based on hierarchical  
477 clustering. The expression of each gene across samples is represented as a row-wise Z-  
478 Score value of the VST-normalized counts from high (red) to low (blue).



480  
481  
482  
483  
484  
485

**Supplementary Figure S12.** Expression across stages in germ cell libraries of the germ cell markers obtained from SLAIDINA *et al.* (2020). Genes are grouped based on hierarchical clustering. The expression of each gene across samples is represented as a row-wise Z-Score value of the VST-normalized counts from high (red) to low (blue).



487  
488  
489

**Supplementary Figure S13** Dot plots of selected proliferation and apoptosis control genes differentially expressed across stages. Expression in VST counts of genes in each tissue-specific RNA-seq library.